## ABSTRACT

## DEPOSITION OF TANTALUM THIN FILMS BY RF SPUTTERING WITH SUBSTRATE BIAS

**by**
**Savita Raina**

The effects of energetic ion bombardment on the crystallographic structure of RF sputtered tantalum thin films on different substrates, particularly aluminum and silicon, have been studied. The effect of substrate biasing on ion current and film thickness has been investigated. The study included comparison between substrate ion current of DC sputtering and RF sputtering and also was aimed at finding the process parameters, which could influence the crystallographic phase of Ta film. The characterization of Ta films is carried by RBS and x-ray diffraction techniques.

A magnetron sputtering system with a matching network between the source and the RF generator has been used to carry out the experimentation. The matching network was adopted from an industrial system and equipped with a manual controller designed and built during the course of this thesis work. Tuning of the matching network allowed stable operation of the sputtering source with RF power of up to 400 W with negligible reflected power (2-3%).

The results of the experiments showed a significant current of ions bombarding the substrate (up to $1.63X10^{15}$ Ions/$cm^2$sec) that increases with negative substrate bias voltage. Significantly higher ion current is observed with RF sputtering than with DC sputtering. With RF sputtering the ratio of ions to atoms arriving at the substrate is larger than 1. Under these conditions and with higher biasing voltage (a few hundred volts) the film thickness decreases due to sputtering of the deposited film by high-energy ions.

XRD results showed that biasing the substrates of aluminum and silicon to -200 V influences the deposition of tantalum films with growth of bcc crystallographic phase (a phase) while films with tetragonal phase (ß phase) grow at lower biasing voltage at room temperature.

This research helped to understand the process conditions for RF sputtering with substrate biasing and its influence on Ta film crystallographic phase. The desired a phase tantalum films have many applications such as in fuel cells, semiconductor industry and as a coating material, which is chemically inert and resistant to corrosion.

# DEPOSITION OF TANTALUM THIN FILMS BY RF SPUTTERING WITH SUBSTRATE BIAS

by
Savita Raina

A Thesis
Submitted to the Faculty of
New Jersey Institute of Technology
in Partial Fulfillment of the Requirements for the Degree of
Master of Science in Electrical Engineering

Department of Electrical and Computer Engineering

August 2005

## APPROVAL PAGE

## DEPOSITION OF TANTALUM THIN FILMS BY RF SPUTTERING WITH SUBSTRATE BIAS

**Savita Raina**

Dr. Marek Sosnowski, Thesis Advisor — Date
Professor of Electrical and Computer Engineering, NJIT

Dr. Haim Grebel, Committee Member — Date
Professor of Electrical and Computer Engineering, NJIT

Dr. Zafar Iqbal, Committee Member — Date
Research Professor of Chemistry and Environmental Science, NJIT

## BIOGRAPHICAL SKETCH

**Author:** Savita Raina

**Degree:** Master of Science

**Date:** August 2005

**Undergraduate and Graduate Education:**

- Master of Science in Electrical Engineering,
  New Jersey Institute of Technology, Newark, NJ, 2005

- Bachelor of Engineering in Instrumentation and Control Engineering,
  Vidyavardhini's College of Engineering and Technology, Mumbai, India, 2002

**Major:** Electrical Engineering

Dedicated to my parents and brother
For their encouragement, support, guidance, immense love and care.

## ACKNOWLEDGEMENT

I would like to thank my mentor and Thesis Advisor, Dr. Marek Sosnowski, for his encouragement, guidance, and support and for an opportunity to work in the fascinating area of thin film deposition and characterization. I would also like to thank my advisor for funding this research partially.

A note of thanks goes to Prof. Haim Grebel for assisting our research team in the Thin Films and Ion Beam Laboratory in carrying out various experiments at the Optical Waveguide Laboratory at NJIT, which really helped me in better understanding of some thin film deposition techniques. I also want to convey my thanks to Prof. Zafar Iqbal for providing guidance during the course of this study.

I would like to express my gratitude to my colleagues Hua Ren and Pradeep Balashanmugam for their immense help during this research. Finally I am highly indebted to my family and friends Mandur, Sarabjit, Saurabh, Rohan and Jyotirmai for their encouragement, patience, support and assistance in all possible ways.

## TABLE OF CONTENTS

## TABLE OF CONTENTS
## (Continued)

**Chapter** **Page**

## TABLE OF CONTENTS
## (Continued)

**Chapter** **Page**

## LIST OF TABLES

## LIST OF FIGURES

## LIST OF FIGURES
## (Continued)

## LIST OF FIGURES
## (Continued)

# CHAPTER 1

# INTRODUCTION

## 1.1 Objectives

The objective of this thesis was investigation of RF sputtering of tantalum, and particularly the effect of energetic ion bombardment of the substrate during the film growth. Effect of different substrates particularly silicon (Si) and aluminum were studied, and conditions which result in deposition of body centered cubic (bcc) α and tetragonal β phases of tantalum, on these substrates were investigated. The deposition of α phase has many applications in particular as protective coatings such as bipolar plates of Al fuel cells. This research was conducted at Thin Films and Ion Beam Lab, at NJIT.

## 1.2 Properties of Tantalum and its Application

Tantalum is an element of group V of periodic table, with atomic weight 180.947, atomic number 73 and density of 16.6gcm$^{-3}$. It is heavy, hard gray metal, which is chemically inert and particularly resistant to most of acids. It exists in two crystallographic phases: ductile, body centered cubic (bcc) α phase with lattice constant $a_0$ = 3.3 -3.4 Å and brittle, tetragonal metastable β phase with lattice constants $a_0$ = 5.3 Å, c = 9.9 – 10 Å. Bulk tantalum exists in bcc form [9] but thin films usually consist of the tetragonal phase or a mix of the two phases. Special conditions are required to obtain pure bcc phase Ta film. The Ta film exhibits different electrical and mechanical properties. α phase has low resistivity (approx. 30μΩ cm) as compared to β phase (approx. 200μΩ cm) [6]. Tough and ductile α phase is usually more desirable than the hard and brittle β phase. Tantalum deposits easer by sputtering than by evaporation due to its high boiling point of 5425 C°. Evaporation is only possible by e-beam sources [10].

Tantalum has different applications both in its pure or compound form. It is used as coating on materials like steel to prevent rusting and provide mechanical strength to stand high temperature wear and erosion. It does not reactant with body fluids and it is also used in making of surgical instruments and implants.

It also has applications in electronics industry [2]. It is widely used in; manufacture of high quality capacitors including those in voltage circuits such as in PDA's, mobile phones etc. It is used in recently developed integrated circuits with copper metallization as a diffusion barrier material between Cu and Si and $SiO_2$ [2], [3], [5] [6] [7]. Films of TaN also have been used in this application. TaN has relatively low resistivity, high temperature stability, mechanical strength, hardness and resistance to oxidation [3].

### 1.3 Thin Film Properties and Application

Thin film deposition techniques play major role in technology. Thin films are extensively used in microelectronics solid state device manufacture, electronic displays such as Liquid crystal displays (LCD), LED's, Plasma and fluorescent displays, optical coatings, magnetic films for data storage and they are also used as mechanical and chemical protective coating.

In application of thin films various material characteristics are considered:

1. Electrical: conductivity of the film, resistivity, dielectric constant, dielectric strength, stability under bias etc.
2. Thermal: coefficient of expansion, thermal conductivity.
3. Mechanical: Adhesion, density, hardness, elasticity.
4. Morphology: Crystalline or amorphous, microstructure, crystalline orientation.

5. Optical: Refractive index, absorption, dispersion etc.
6. Magnetic: Saturation flux density, permeability.
7. Chemical: Composition, impurities, etch rate, stability, impurity barrier or gettering effectiveness.

### 1.4 Thin Film Deposition Techniques

Thin Film Deposition is carried out by various methods. The figure 1.1 shows the classification of thin film deposition techniques:

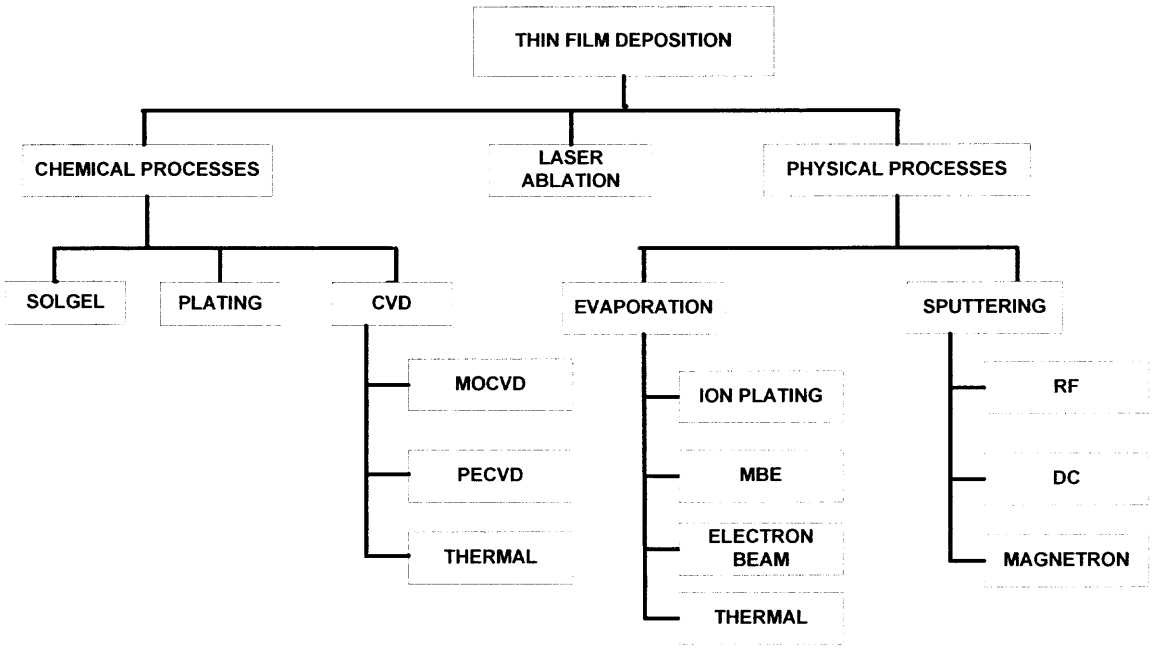


**Figure 1.1** Thin film deposition classifications.

Thin film deposition is broadly classified into physical vapor deposition (PVD) and chemical vapor deposition (CVD). CVD is a process of deposition of volatile compound of a material on substrate; to produce a non-volatile solid that deposits its atoms or molecules on suitably placed substrate [11]. Whereas PVD process involves a

controllable transfer of atoms or molecules from a source to substrate. PVD has some advantages over CVD which include:

1. Ability to deposit good quality thin films at low process temperature without substrate heating
2. Eliminates hazardous gases and chemicals, which help to provide safety.

Evaporation and Sputtering are the two main methods of physical vapor deposition. Evaporation is a process by which atoms are removed from the source by thermal energy, where in sputtering the atoms or molecules that form film are ejected from the target material by bombarding it by energetic ions.

Evaporation is the simplest thin film deposition technique. This process has some advantages such as high deposition rate, simplicity, and ease of use. Vacuum evaporation is used for thin films in manufacture of some electronic circuits, and devices, for application of optical coatings, and for developing technologies such as high temperature superconductors [12]. This is a thermal, low energy process. Sputtering is an important PVD technique described in detail in chapter 2.

# CHAPTER 2

# SPUTTERING

## 2.1 Principle of Sputtering

Sputtering is a process where the atoms that form the film on a substrate are obtained by bombardment of the target by energetic ions in partially ionized rare gas (plasma) composed of ions, and electrons. These ions are produced in the chamber by applying high voltage between the electrodes at low pressure. Ions from rare gas discharge eject or sputter atoms from the target material. The properties of the films produced by this process are dependent on the gas used, target material, power applied, gas pressure, and system geometry.

Sputtering is widely used for elements including titanium, tantalum, niobium etc. since all these have high melting point. It is also used for metal like aluminum, which is used for interconnects in semiconductor device fabrication [25]. Sputtering is a technique, which makes use of plasma, so brief description of plasma is given below.

Plasma is ionized gas containing equal number of positive ions, and negative electrons. The presence of charged particles makes plasma conductive. These charged particles are produced by placing high voltage across the electrodes, in presence of gas in medium vacuum range (< 1 torr). In plasma there is constant change of energy, and momentum between the particles. The speed of electrons is much larger than that of ions due to their lower mass (mass of proton is 1837 times mass of electron). When an object is placed inside the plasma it develops negative charge since electron current density in the plasma is more than that of ions. This process of building of negative charge continues till the negative potential on the object starts repelling any more incoming

electrons. This potential is equal to the "plasma potential", a potential of the plasma, which is more positive than the potential of the object, and the container it wells. The contact potential in the plasma decreases to zero exponentially, thus plasma beyond a distance λ is essentially shielded from the effects of external charges. This distance λ is called as Debye's length [29]. The plasma is characterized by glow discharges due to excitation of the atoms and molecules of gas followed by radiative excitation with emission of particles in visible and UV spectrum range. One exception to this is cathode dark spaces where few electrons are present, hence not many electron–atom collisions, therefore not much excitation of electrons so low luminosity.

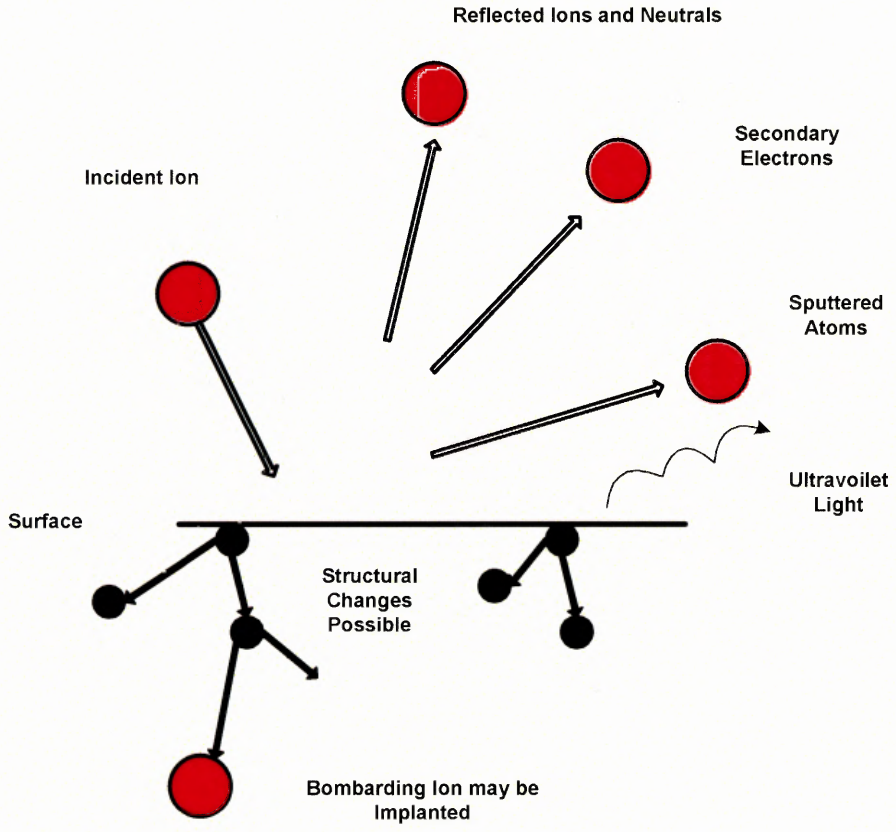


**Figure 2.1** Interaction of ions with surface [14].

The mechanism of sputtering is explained with the help of Figure 2.1. The energetic ions when incident on the target surface lead to various different phenomena. The ion may strike the target and get reflected back in form of neutral atom or an ion. This phenomenon also leads to generation of secondary electrons, which are ejected out by an electron, ion, photon or neutral. Secondary electrons generally have energy less than those of incident particles helping to maintain the glow discharge.

The incident ion can lead to structural rearrangement of the target material, generation of vacancies, interstitial and changes in electrical charge levels. The incident ion can be buried in the target material. This phenomenon is called "Ion Implantation" which is applied for doping of the silicon wafers to manufacture integrated devices. Lastly it can lead to sputtering; where this ion ejects the atoms of the target material, which can get deposited on the substrate.

Sputtering atoms coming to substrate have energy of few eV (higher than evaporation). The substrate is bombarded by energetic electrons, neutral particles, and photons. These energetic particles can lead to damage in the substrate.

## 2.2 Types of Sputtering

Sputtering can be accomplished by diode, magnetron, RF or DC sputtering methods. These methods are explained in details in the following subsections.

### 2.2.1 DC Sputtering

Within the sputtering process, gas ions of the plasma are accelerated towards the target consisting of the material to be deposited on the substrate. A DC sputtering consists of two electrodes i.e. cathode and anode placed in vacuum chamber. In this particular

sputtering technique, negative voltage is applied to the cathode (target electrode) whereas anode (substrate) is generally grounded, electrically floating or biased [12]. The chamber usually uses Argon gas (noble gases are used because they do not react with the target material) introduced in the chamber at a pressure as high as 1 torr initially and later after the glow discharge is stabilized the pressure can be maintained at few - 100 mTorr. Positive ions in the discharge strike the cathode plate and eject neutral atoms. These atoms flow in the plasma and strike the substrate and get deposited. The number of atoms or molecules sputtered from the target depends upon the ions that strike its surface. DC sputtering is generally used for conductive materials

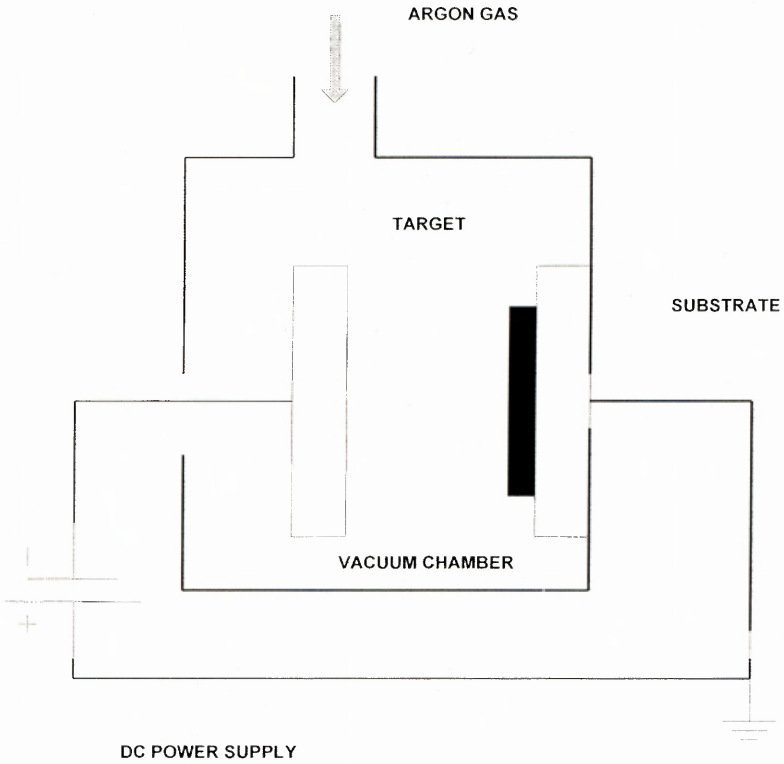


**Figure 2.2** DC sputtering [14].

### 2.2.2 RF Sputtering

DC sputtering was used to deposit conductive materials where a negative voltage was applied to the target. There arose a need to deposit insulating thin films or films of non-conductive material. That is where RF Sputtering came into picture, though this technique is now used even for conducting materials.

There are added advantages of RF apart from being used for insulating films, such as:

1. It is more efficient in maintaining discharge and in promoting ionization.
2. At higher frequencies at which it is generally used (>1 MHz), the operating pressure can be decreased.
3. For a given pressure, impedance of the discharge decreases with increasing frequency, so more current can be drawn through the discharge at given voltage [14]

This process uses alternating current (AC), which neutralizes the charge build up on the insulating plate. When negative potential is applied to the target, it is bombarded by positive ions and since the target is insulating the positive charge keeps on building on the target until it repels any further positive bombardment. Later during the positive half of the cycle it is bombarded by electrons and thus neutralizes the target. Frequencies of 1 MHz or more are required for producing continuous discharge. For the flow of alternating current at these frequencies insulating target is equivalent to a dielectric of a series capacitor.

Standard RF frequency for industry allocated by international communication authorities is 13.56 MHz, so that it does not interfere with communication. RF plasma impedance must be matched to the standard 50Ω ** impedance of RF generator. Plasma impedance changes with the process conditions (The plasma impedance greatly depends

upon the plate area, spacing, gas type, pressure and temperature.). Therefore an impedance matching network is needed so that load inside the chamber appears as 50 Ω to the RF generator. This is done to ensure minimum power is losses.

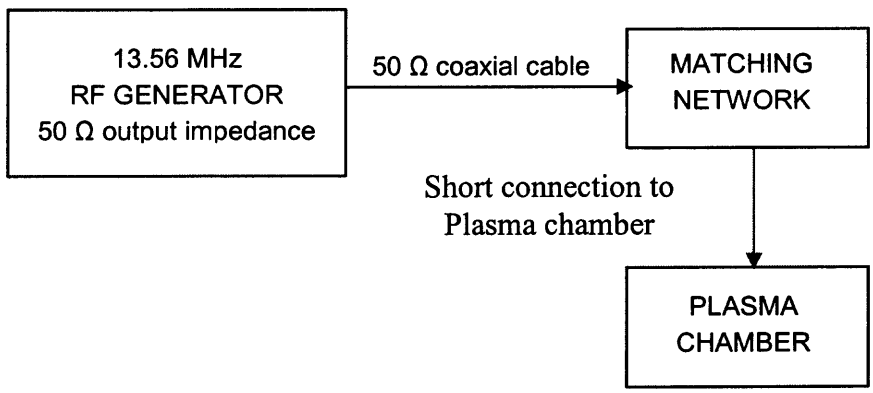


**Figure 2.3** Block diagram of RF power transfer to the process chamber.

### 2.2.3 Ion Beam Sputtering

Ion beam sputtering is a thin film deposition technique where ions, which help in film formation, are generated externally by ion beam source using noble gas. Substrate is placed in high vacuum field free surrounding. The simple arrangement for this technique is shown the figure 2.4

The yield of atoms and molecules is less as compared to evaporation but the deposition material has higher kinetic energy than evaporation, which helps in better nucleation of the film. This improved nucleation enhances the properties of the film like adhesion, lower mechanical stress, increased packing density. [39].

** 50Ω coaxial cable is very widely used with radio transmitter applications. It is used here because it matches to many common transmitter antenna types, can quite easily handle high transmitter power and is traditionally used in this type of applications (transmitters are generally matched to 50 ohms impedance)

This method is limited to some materials like semiconductors, oxides, metals etc.

The various advantages of this technique are listed here:

1. Insulators can be sputtered without charging them. Control of process is improved greatly with ability to control incident angle and beam current.

2. The process requires low chamber pressure ($10^{-4}$ Torr) so in a way contamination due to gas is minimized.

3. Substrates are isolated from glow discharge so unwanted heating of the substrate is minimized.

4. Substrates are not part of electric system so control on process parameters like heating, cooling is easier.

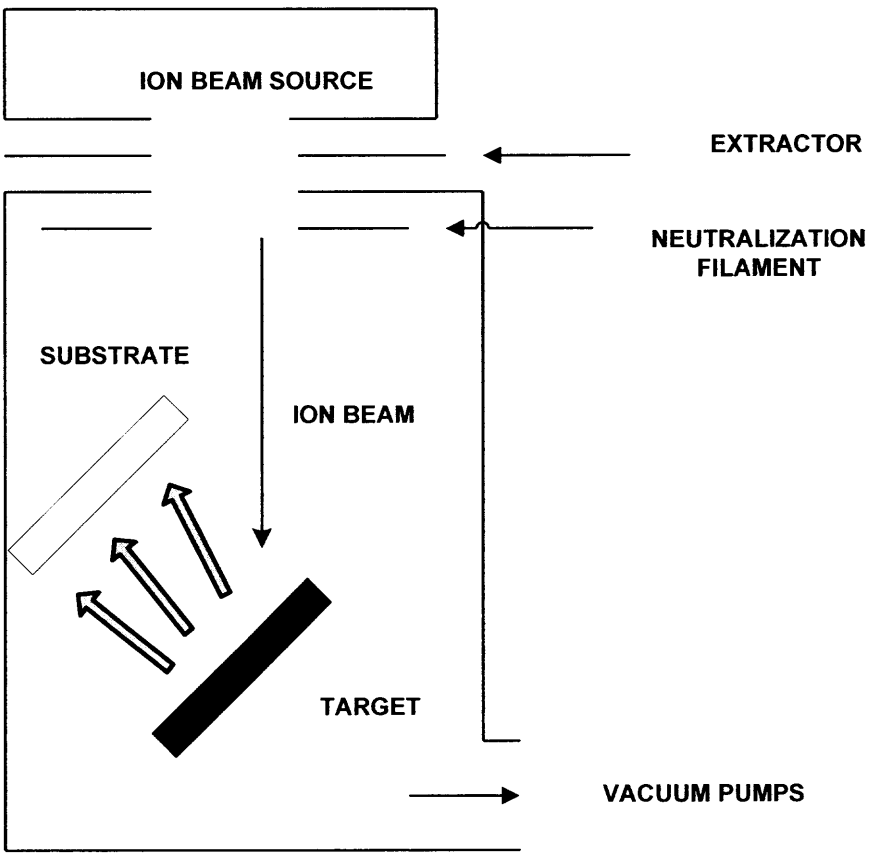


**Figure 2.4** Ion beam sputtering [14].

## 2.3 Ion Beam Assisted Deposition

Ion beam assisted technique is a physical deposition technique of direct deposition of the ions of low energies for thin film formation. The nature of the process enables deposition of coatings having a wide range of metallurgical compositions, and with a high degree of control over nanostructure [24]. This technique allows deposition for variety of optical, dielectric and semiconductor materials. This technique is similar to ion beam sputtering except that here instead of using noble gas ion beam, beam of material to be deposited is used. This beam of material is allowed to deposit on substrate [14]. The process allows deposition of wide range of coatings with high level of process control, which assists in better film growth. This deposition process can be carried also by evaporation or sputtering.

Low temperature thin film deposition techniques can lead to inferior film growth. This technique can be applied with sputtering, evaporation or ion plating to achieve better film quality. Energetic ion bombardment greatly affects the film adhesion, morphology, stress, more uniform growth and controllable composition. The instrument arrangement is similar to that of ion beam sputtering with substrate placed instead of target as shown in Figure 2.4 ion beam is directly directed on the substrate.

This technique is categorized into two types based on the type of reactive species. The first type is a reactive technique in which plasma contains activated nitrogen or oxygen atoms that react with substrate to form compounds for example in production of nitrides and oxides. In non-reactive technique, ion beam assisted deposition energy is a parameter, which needs consideration. Here ion energy and flux density of the ions are considered.

## 2.4 Magnetron Sputtering

There are two types of sputter source: diodes and magnetron. These can be supplied with either RF or DC power. In diode source the target is in form of flat disk for which external power is supplied. Diode sources are cheapest and are least complex sputter sources available but these sources have certain disadvantages such as they do not make efficient use of generated electrons for maintaining plasma, secondly deposition rates are higher in magnetron sputtering than diode sputtering [12].

In simple DC sputtering electrons are lost due to recombination with the walls and other ions in the chamber as a result the glow discharge diminish down. To improvise this system, magnetrons were introduced. Magnetrons increase the path length of the electrons before they get collected at anode or recombine with the walls of chamber. It also enables electron to cause more ionization of the gas. This also helps to prolong the plasma in the chamber [14]. The principle of these magnetrons is explained as follows.

A charged particle q with mass m and velocity v when placed in magnetic B experiences a force F perpendicular to both its motion and direction of magnetic field B. This is shown in figure 2.6 where the field is into the paper. This force F is known as Lorentz force and is given by the equation:

$$F = q\,(v \times B) \tag{2.1}$$

At the same time this charge particle also experiences motion due to Centrifugal force Fc. This force is given by the equation 2.2

$$\text{Centrifugal force } Fc = mv^2 / r \tag{2.2}$$

From equation 2.1 and 2.2 we conclude

$$r = m\,v/q\,B \tag{2.3}$$

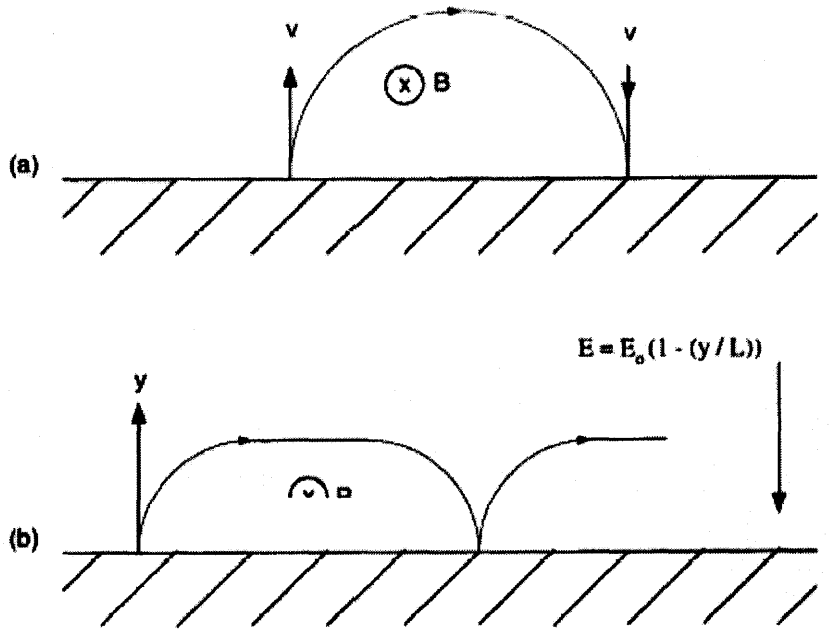


**Figure 2.5** Motion of an electron ejected from a surface with velocity v into region of magnetic field B parallel to the surface
(a) with no electric field
(b) with a linearly decreasing magnetic field [14]

The charge of electrons and ions is same but their difference in masses produce difference in the radius of their movement. According equation 2.3 radiuses is directly proportional to mass hence radius of ion is almost 1837 times of electron. Figure 2.6 (b) explains the actual situation in magnetron sputtering systems. To understand it better, consider Electric field E, which decreases linearly across the dark space of thickness L and magnetic field B parallel to the surface of the target. Let y be the dimension away from the target, when y = 0 then Electric field is given by the equation 2.4

$$E = E_0 (1 - (y/L)) \tag{2.4}$$

When emission velocity is zero then y is given by equation 2.5

$$y = q E_0 / m_e \omega^2 (1 - \cos\omega t) \tag{2.5}$$

When E = 0 then ω is equal to qB/ $m_e$, which is known as cyclotron frequency. The presence of electric field, changes the orbit of motion of the charged particle from circular to cycloidal [11].

The main purpose of using magnetic field near the target on magnetron is to keep the electrons close to the target. The electrons generate more ions by its impact on the target. Due to a higher plasma density near the target the deposition rate increases. The disadvantages of these sources are that they are more complex and expensive than simple diode source and also lead to uneven consumption of the target material. [12]. Magnetrons are also used in RF sputtering though they are not as effective as in case of DC sputtering because of fluctuating electric field and less confinement of electrons. [14].

## 2.5 Reactive Sputtering

In reactive sputtering thin film of compounds are deposited on substrates by sputtering from the solid targets in presence of a reactive gas, usually mixed with the inert gas (Ar). This results in a compound of reactive gas and the target material. The most common compounds sputtered by reactive sputtering are [8] follows:

1. Oxides (oxygen) – $Al_2O_3$, $In_2O_3$, $SnO_2$, $SiO_2$, $Ta_2O5$
2. Nitrides (nitrogen, ammonia) – TaN, TiN, AlN, Si3N4
3. Carbides (methane,acetylene,propane) – TiC,WC,SiC
4. Sulfides ($H_2S$) – CdS, CuS, ZnS
5. Oxycarbides and oxynitrides of Ti, Ta, Al and Si.

The problem with reactive sputtering is that these reactive gases react with the target material and form its compound on the surface resulting in low deposition rates. In extreme cases this problem will result in instabilities such as sparks or extinguishing of plasma [31]. One of the remedies for this is to increase the gas flow and the pumping rate of the chamber.

# CHAPTER 3

# DEPOSITION EQUIPMENT AND EXPERIMENTAL PROCEDURE

## 3.1 Deposition Equipment

This chapter describes the deposition equipment, modifications and the procedure followed to carry out the deposition of Tantalum films on different substrates such as Al, $SiO_2$/ Si, Glass, and Steel. Deposition is carried using Magnetron Source supplied by RF power with substrate biasing.

The equipment for this research consists of cylindrical stainless steel vacuum chamber of 80-liter capacity. Height of chamber is 15" and the diameter is 20". The chamber is covered by a lid and this lid is moved up and down with the help of motors. The picture of this unit is shown in Figure 3.1.

Chamber is supplied with Magnetron source Torus 2 obtained from Kurt J Lesker Company having planar geometry. The source is mounted inside the chamber on a tubular support, which has compression vacuum feed through which allows its vertical movement. The distance between target and source can be adjusted between 3" and 6". Magnetron source is water-cooled and is mounted in the chamber for sputtering process. Water-cooling of source is provided to avoid overheating of the target and also to prevent damage to magnets of the source. Magnetron source is connected to the RF power through coaxial cable of 50Ω impedance. Tantalum is used as target material and it comes in to two diameters viz. 0.125" and 0.25" of 99.99% purity. Provision is made to avoid the sputtered material to deposit on the chamber walls by placing a steel shield mounted on four poles, placed above the source (target). Above this steel shield, a shutter

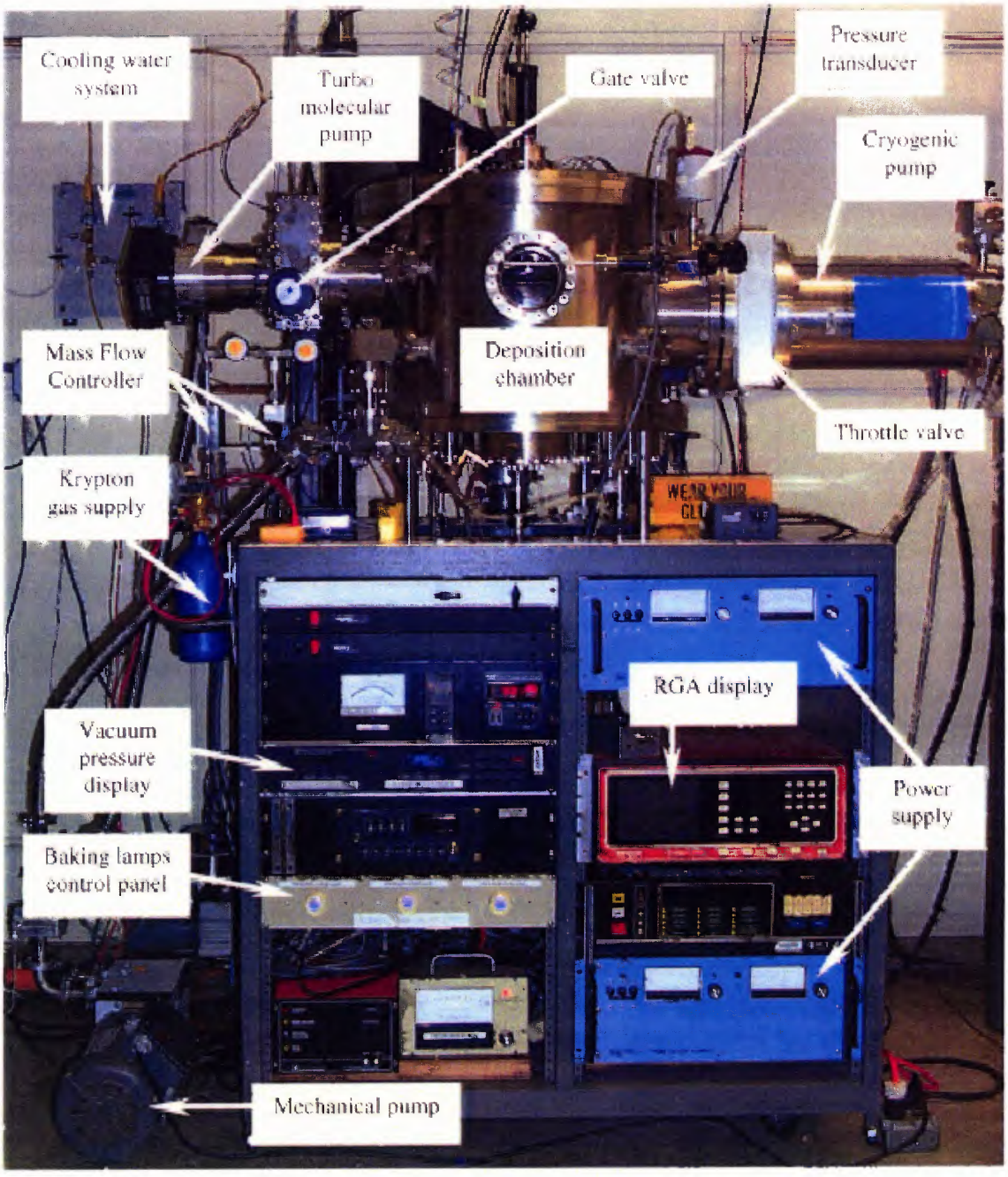


**Figure 3.1** DC magnetron sputtering System [33].

Constructed from stainless steel is placed, which is used to cover the source when the substrate holder position is changed to prevent deposition on other substrates.

The substrates to be sputtered are mounted on a circular plate of 16.5" diameter shown in the figure 3.2. Eight substrate holders can fit in this open circular plate.

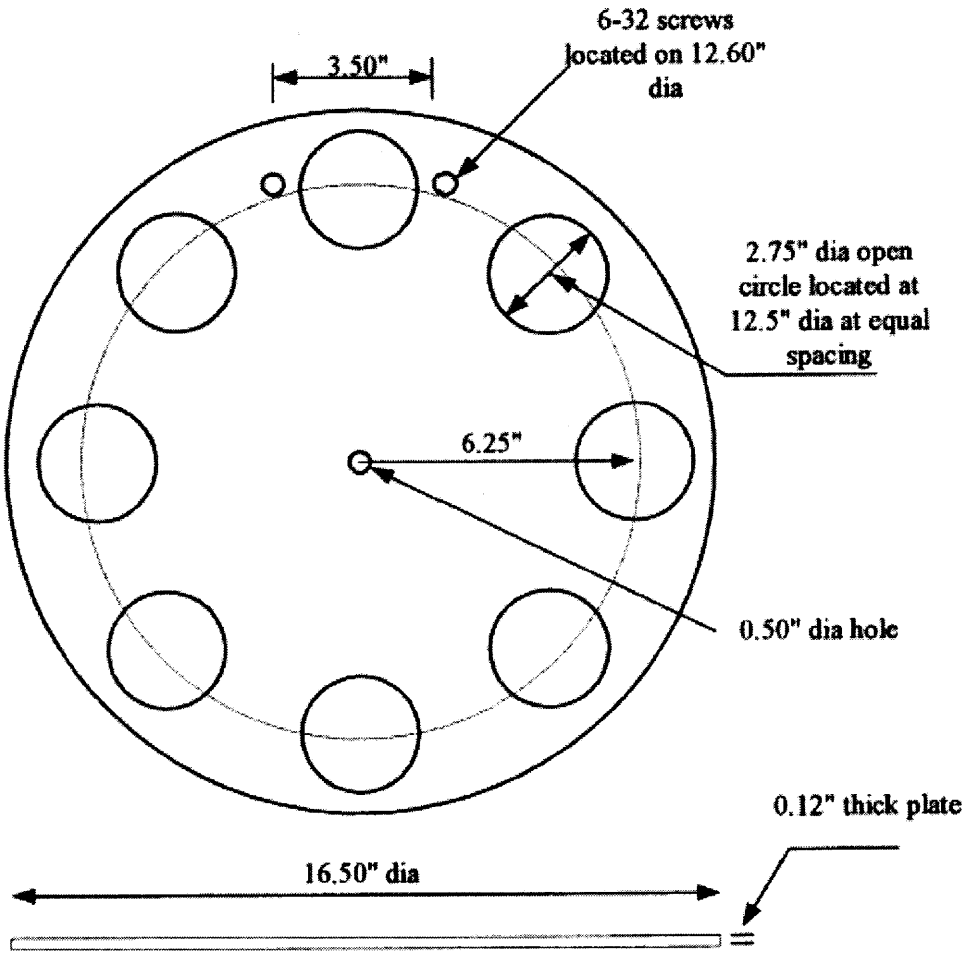


**Figure 3.2** Dimensions of substrate holder plate [12].

The substrates are mounted above the source so that particle or flakes from the target material do not fall on the substrates, which can greatly effect the film deposition. This plate is mounted in center of the lid of the chamber and manual control for

movement of the plate is facilitated on the chamber. A shield with a circular opening below the substrate plate assures that at one time only one substrate holder plate is exposed to the sputtering source.

The substrate holders are made from stainless steel and different substrates are attached to the holder using stainless screws. This is shown in figure 3.3. The substrate holders can be electrically isolated from the substrate plate by ceramic insulators. This was used for biased sputtering to investigate effect of ion bombardment.

**Figure 3.3** Substrates holder with screws which hold the substrate [31].

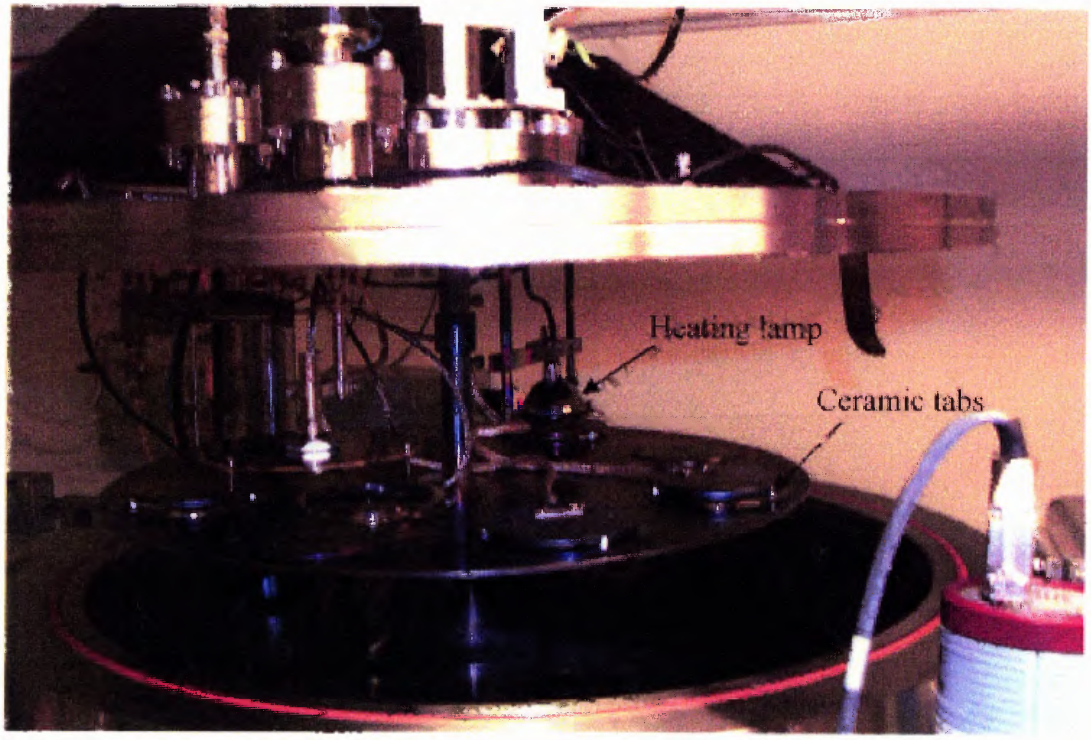


**Figure 3.4** A view of the deposition chamber from top, showing plate with substrate holder [31].

A thermocouple was attached to one of the substrate holders and another to the substrate plate to monitor the temperature during deposition. To measure high vacuum pressure, ionization gauge is attached outside the chamber. Argon gas pressure inside the chamber is measured by capacitance manometer (pressure transducer MKS Baratron.) of range 0 -1 Torr. Pure Argon and Nitrogen are used to carry out sputtering procedure. Flow of these gases to chamber is controlled by mass flow controllers (0 -100 sccm).

It is necessary to keep the chamber moisture free and this is done by baking the chamber at about 150 $^{o}$ C for 6 – 8 hours. For baking the chamber two elongated halogen lamps (500 W, 120 V) have been placed inside the chamber. Substrate heater is also provided inside the chamber to carry deposition at higher temperatures.

The chamber is equipped with a CRYO – TORR 8 high vacuum pump from CTI Cryogenics, Helix Technology Corporation. It is also supported by Turbo molecular pump from Turbovac 50 ( Leybold – Heraeus). To reach the required fore vacuum for operation of turbo or CRYO pumps mechanical pump is used. Fore vacuum is measured by the thermocouple vacuum gauge where as high vacuum is measured by ionization gauge. The system is also equipped with residual gas analyzer (Inficon Quadrex – 200 Model from Leybold – heraecus). RGA is used to analyze the composition of the gas inside the chamber. CRYO- TORR pump and RGA were not used for this study.

### 3.2 Modified Sputtering System

The sputtering system at Ion Beam and Thin Films Lab was constructed keeping in mind DC Magnetron sputtering for tantalum. This study was aimed at investigating RF sputtering of Tantalum with substrate bias, so certain modifications had to be made in the deposition system. This work included:

1. Modifying RF tuning network and building a manual tuning controller for supplying RF power to the sputtering source.
2. Power substrate holder connections to DC biasing.

RF generator generates frequency of 13.56 MHz and this frequency is fed to the source. It has two analog meters, one show the RF power supplied and other shows the reflected power. This system from Omega model # RFG - 1250 came along with an automatic matching network for impedance matching.

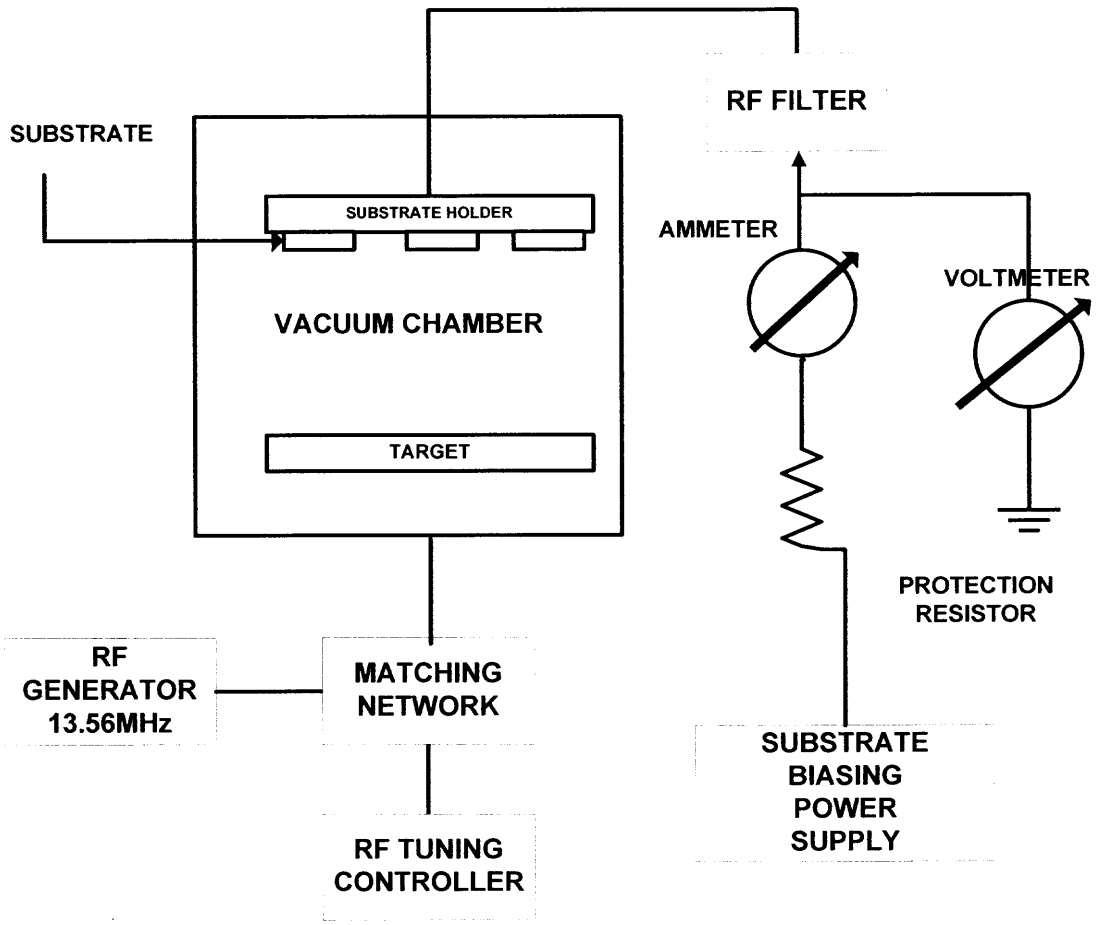


**Figure 3.5** Block diagram of RF Power connection to the sputtering source with substrate biasing.

This matching network could not match the impedance of the generator with that of source torus 2 so, an adopted matching network from Advanced Energy model # M/N 5017-000-01 with manually controlled RF tuning network was introduced, which is explained in section 3.2. The schematic of the original matching network is shown in the Figure 3.6

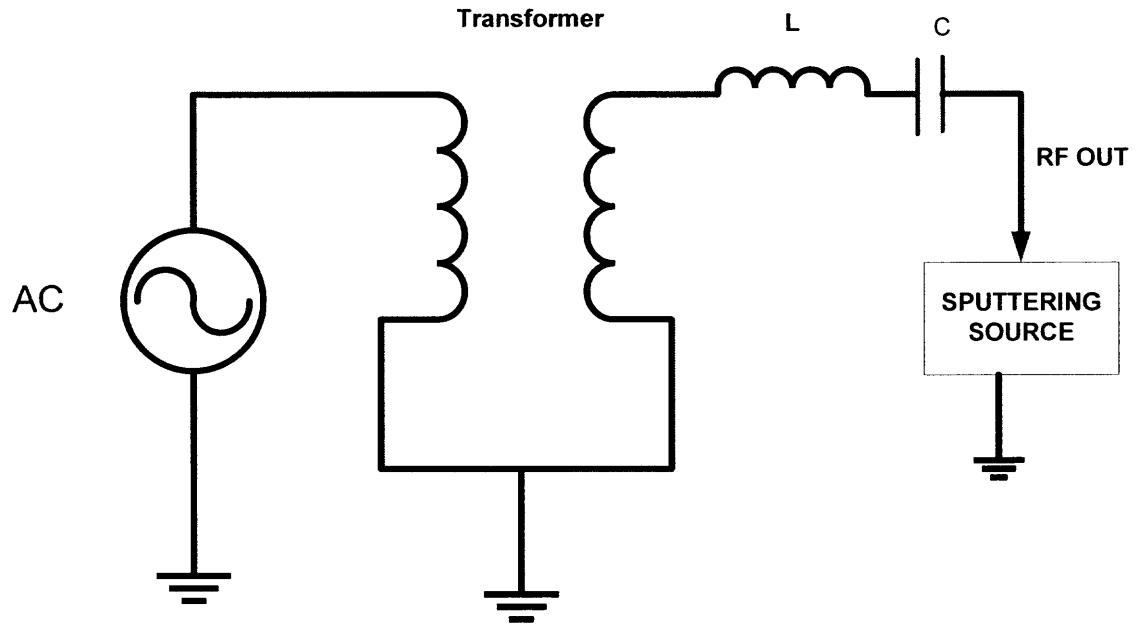


**Figure 3.6** Original matching networks from Omega.

This matching network consists of a transformer, an inductor and 60 pF capacitors. The RF output from this circuit is directed to the plasma chamber.

For proper installation of the matching network some rules were followed. The unit should be properly enclosed so as to protect the circuit inside the network from behaving erratically. The first consideration is that matching network should be as close to vacuum chamber as possible to minimize impedance between the sputtering unit and RF generator. Good ground connections between the RF unit and matching network are required. Proper grounding helps to prevent electromagnetic interference and radiations. It also ensures equipment safety and personnel security.

### 3.2.1 Adopted Matching Network

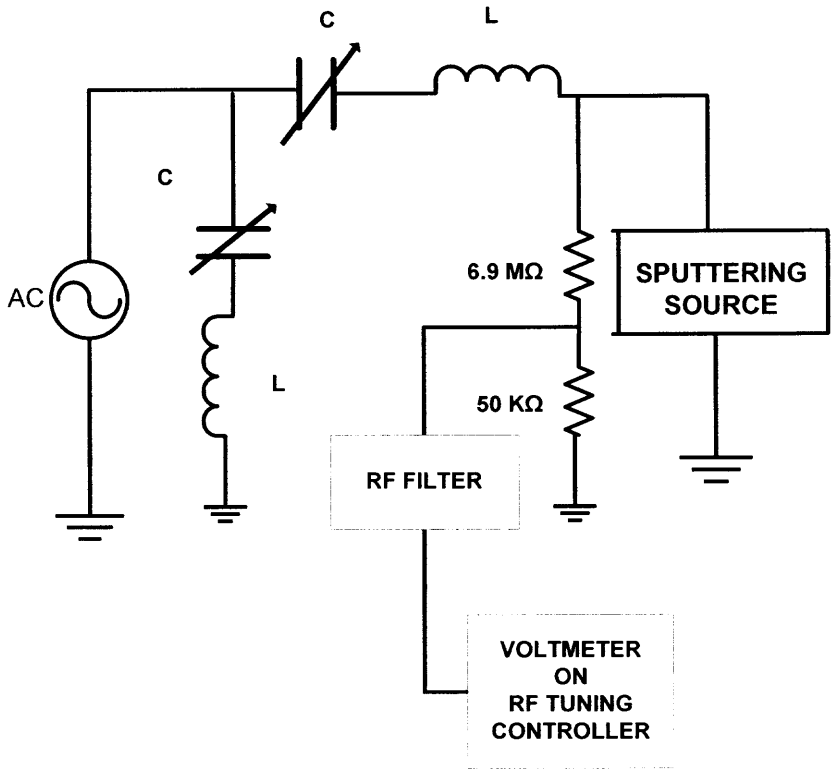


**Figure 3.7** Adopted matching network from Advanced Energy.

Matching network is to overcome the impedance mismatch between the RF generator and source (in this study torus 2). The matching network converts the complex impedance of the operating source to a resistive load.

This adopted unit consists of two variable capacitors and two inductors. These two variable capacitors are driven by 6-volt DC motors. For position sensing two 10 K potentiometers are attached on the shaft. A voltage divider is added, which is attached to the source and the output is fed to RF filter, which gives the DC voltage developed on the source. This voltage is read on the ammeter in terms of current.

### 3.2.2 RF Tuning Controller

This unit was constructed and designed to tune the matching network from Advanced Energy, which control motors for tuning of variable capacitors in the matching network. This unit can be divided into two circuits

1. Tuning of motors which control movement of the variable capacitors
2. Measure the DC voltage developed on the electrode.

The first circuit of tuning controller gives us the relative position of the capacitors in terms of voltage V1 and V2 shown by the analog meters on the front panel of the RF tuning controller. The scale of voltmeter is from 0 – 15 volts. For this circuit two 10 k potentiometers were used separately in series with two 1.85 k resistors. The value of potentiometer where maximum deflection of 15 V from 11 V battery supply was attained when potentiometer is fixed at variable point of 9. 16 – 9.29 kΩ. The meters are connected to 11-volt supply. Here in this arrangement the positive terminal of the meter is grounded and negative terminal is connected to the rest of the circuit. The schematic of the RF tuning controller unit is shown in figure 3.8

The second circuit placed in the RF tuning controller for measurement of DC voltage developed during biasing. This circuit consists of 741 op-amp, which is used as voltage follower. An ammeter of 2k resistance and scale of 0 – 1 mA is used to read the DC voltage developed during biasing on the electrode. This voltage is read in terms of current and the system was calibrated, according to which 0.2 mA of current is equal to 500 V DC on electrode. The voltage from the electrode comes through the voltage divider and RF filter in the matching network to the op-amp circuit through a potentiometer.

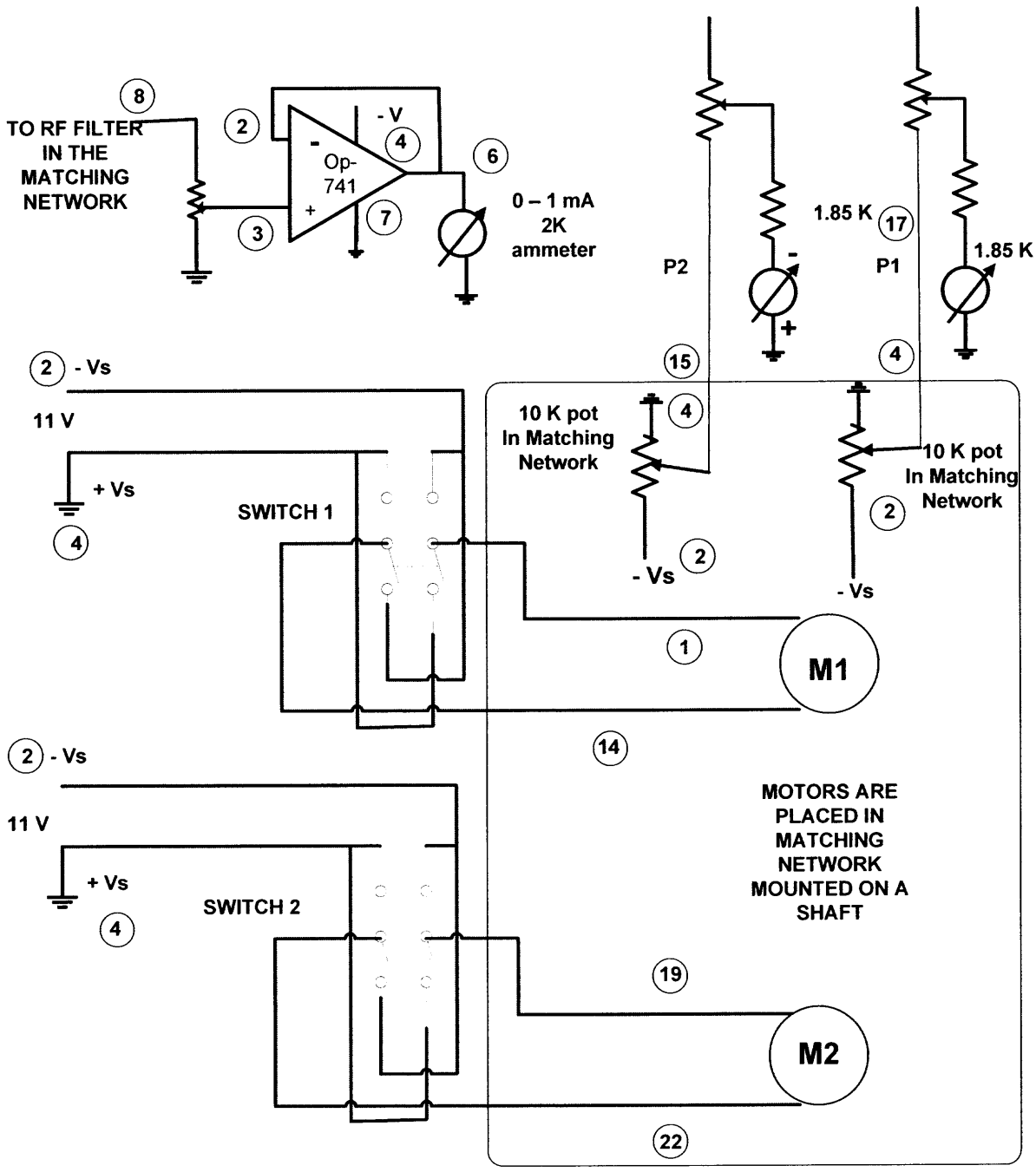


**Figure 3.8** Schematic of RF tuning controller.

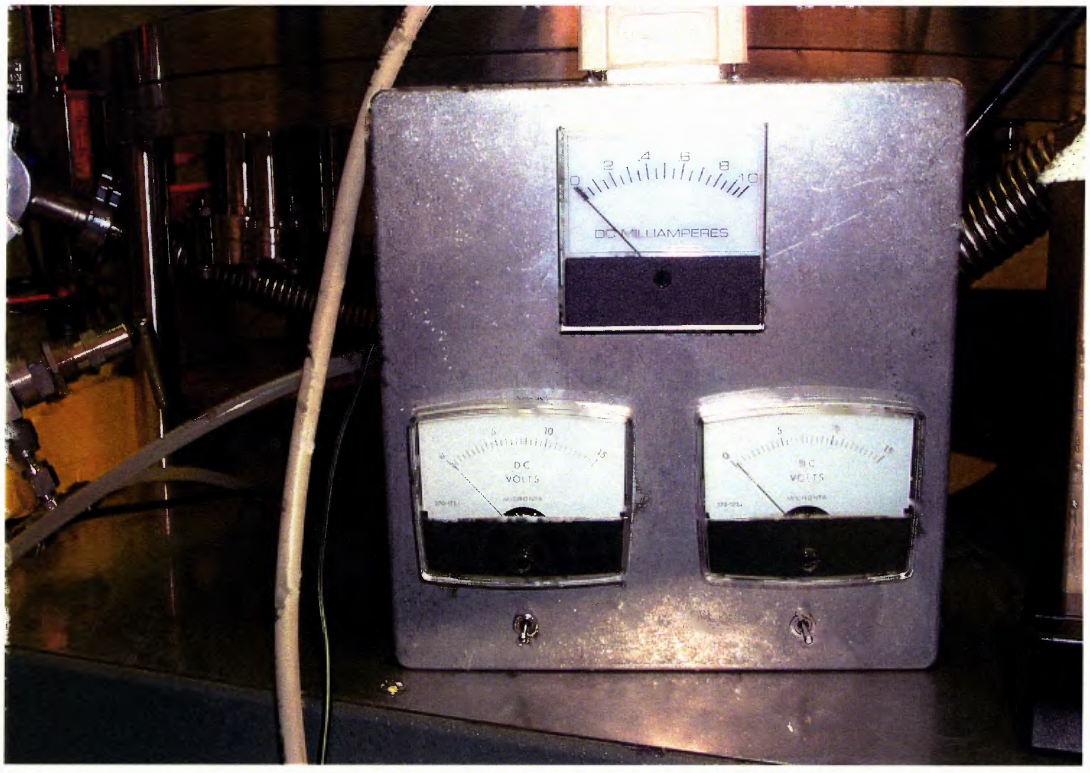


**Figure 3.9** RF tuning controller.

The RF filter is attached so as to filter out the radio frequency interference, which greatly affects voltage readings. The circuit diagram of this circuit is also shown in the figure 3.8

### 3.3 Procedure for Deposition

To carry out deposition of the thin tantalum films the following procedures were followed. The substrates, on which deposition is to be made, need to be cleaned. This is a very important step because it helps to accomplish better bonding between the deposited material and substrate. This is done by ultrasonic cleaning. First step in ultrasonic cleaning is to clean the substrate in alcohol for 10 minutes. Then put them back in acetone and do it again for 10 more minutes. Finally substrates are put back in alcohol and cleaning is again done for 10 minutes. In some experiments substrates were dipped in HF solution followed by putting them in distilled water.

Substrates are mounted on the substrate holders and loaded in the chamber. All connections are checked. Connector from a biasing feed through to a stainless steel spring making contact with substrate holder, which comes to the position above the target are checked. The substrate holders are isolated from the substrate plate by using ceramic beads (3 in number).

Chamber is closed and pumped first by mechanical pump. Fore vacuum should reach few 1 hundred mtorr to start the Turbo pump. After few hours of pumping the vacuum should reach in range of 1 X $10^{-5}$ torr and after over night pumping it reaches 1 X $10^{-6}$ torr. The chamber is baked usually baked overnight to get rid of moisture and this is explained in detail in section 3.1.

To start deposition process rare argon gas is allowed to flow through the chamber at rate of 18 sccm controlled by mass flowmeter. Care should be taken that ionization gauge is put off during this process. The RF generator is turned on and to initiate plasma argon pressure of few hundred mtorr is needed. After plasma is initiated pressure is adjusted by partially closing the gate valve to the turbo pump. The pressure in the chamber is read by MKS baratron transducer. Controller is adjusted so that minimum power is reflected back by the source. The deposition is usually carried out for 10 minutes for each substrate holder. After deposition is completed, the chamber is allowed to cool and chamber is fed by nitrogen gas to open up the chamber and finally the substrates are removed from the substrate holders. Some deposition were carried out at higher substrate temperature of 400 $^{0}$C to see if temperature effects the phase change, for that substrate heater were used.

# CHAPTER 4

# CHARACTERIZATION TECHNIQUES

This chapter explains various experimental techniques for analysis of the substrates like silicon dioxide, silicon, aluminum, steel and glass. The characterization of the thin film material is done for parameters such as film thickness and film composition. Determining film thickness is an important measurement because the properties and behavior depends upon thickness. Film composition is also a very important parameter that needs attention because this study aims at effect of RF sputtering and substrate biasing on phases of Tantalum and the intensity of these phases obtained on thin film. For the study of these two parameters, X ray diffraction (XRD) and Rutherford back scattering (RBS) have been used. These two characterization techniques are explained in detail in the following sub sections.

## 4.1 X Ray Diffraction

X-Ray diffraction is a versatile, non-destructive technique used for determining the crystalline phases (stress, grain size, crystal orientation, phase composition, defects) of the material. This process is helpful for the study of crystals because the wavelength used in this process is close to the spacing between the atomic planes of the crystal causing its diffraction.

The instrument for X ray diffraction consists of X ray generator, detector for detecting the scattered beam a diffractor and a computer, which has a library of references of diffraction patterns from various substrates. In this technique, an x-ray beam travels through the material, which causes diffraction due to scattering of x-ray by the crystal. This scattered beam from the successive planes is then collected by x-ray

detector for analysis. Since the diffraction pattern created is a characteristic of any particular material, the data collected is fed to the computer attached to the x-ray instrument to identify the material.

This technique is based on Bragg's Law, which can be explained in form of an equation 5.1 and can be intuitively shown in figure 4.1.

$$n\lambda = 2d \sin\theta \qquad (5.1)$$

n = n is an integer
d = variable *d* is the distance between atomic layers in a crystal
$\lambda = \lambda$ is the wavelength of the incident X-ray beam
$\theta$ = X-ray beams at certain angles of incidence

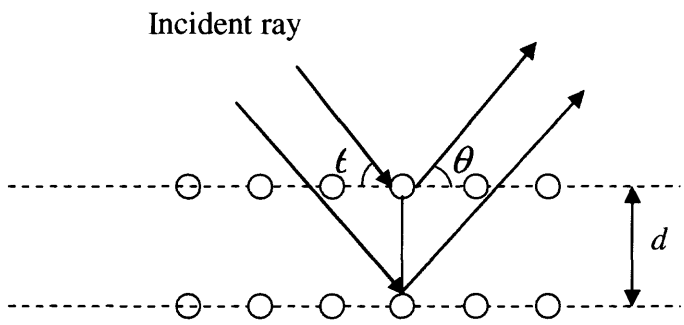


**Figure 4.1** Bragg' diffraction principle.

In this study XRD was used to determine the quantity of α and β phases on the thin film in terms of intensity of particles and intensity is measured in counts per second (cps). XRD measurements on different substrates were performed using Philips X'pert MPD instrument with Cu Kα radiations in which monochromatic X- ray source was set at

20 kV and 10 mA and the scanning angles 2θ (from 20 degree to 110 degree.). The schematic of Philips X'pert is shown in the figure 4.2

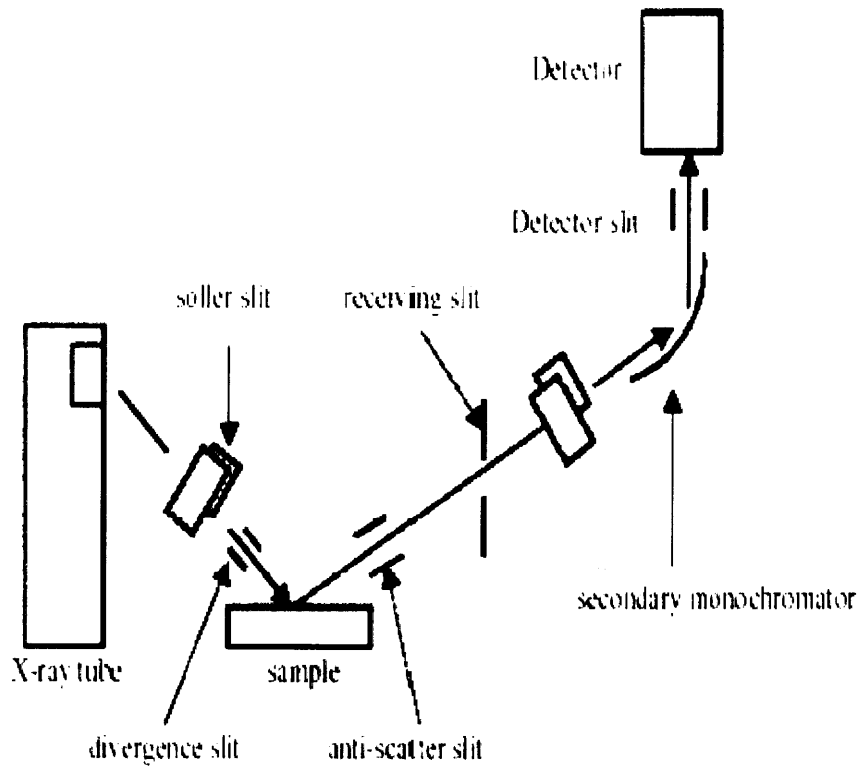


**Figure 4.2** Philips X'pert instrument schematic [31].

XRD spectra obtained from the instrument were compared with standard spectra of Ta bcc α and Ta tetragonal β phase, shown in the figure 4.3 and 4.4 respectively. Also XRD measurement of substrates were taken viz. silicon, steel, Aluminum were taken.

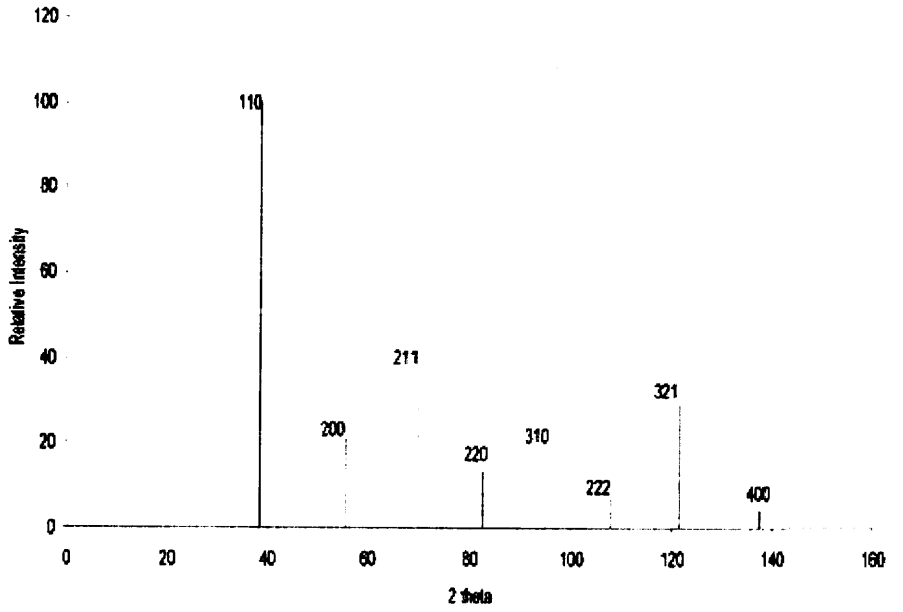


**Figure 4.3** Standard powder diffraction spectra for bcc tantalum [18].

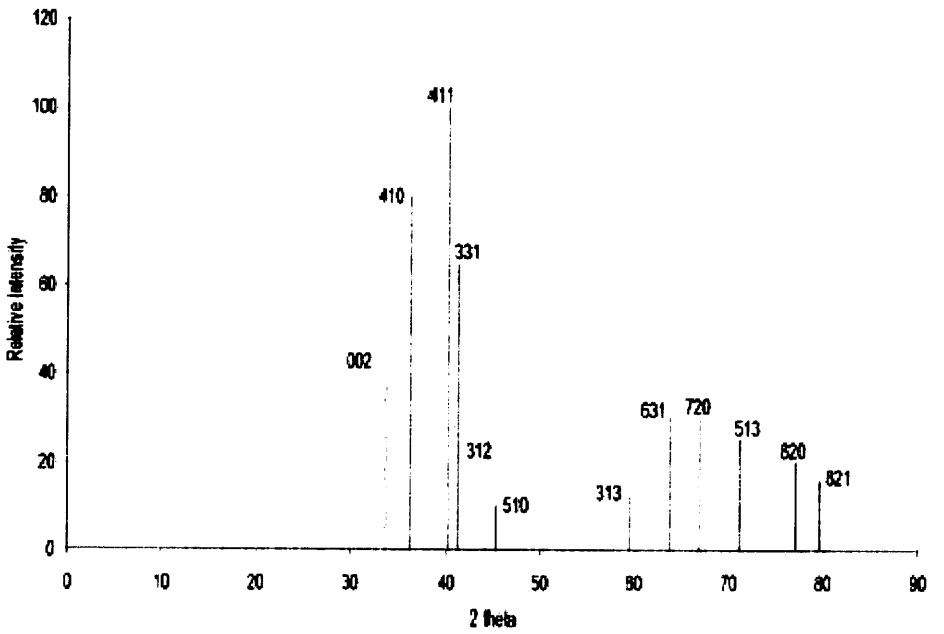


**Figure 4.4** Standard powder diffraction pattern of beta tantalum [19].

## 4.2 Rutherford Back Scattering

Rutherford back scattering is a non-destructive technique with no consideration to charge transfer and sputtering. In this technique the energetic (MeV energy) ions of low mass are bombarded on the sample. As the result, these energetic ions penetrate the sample and are reflected back from the surface. There are electronic collisions, which take place at the surface or inside the sample, energy losses through out the depth. By the fundamental principle of conservation of energy and momentum, these ions lose energy primarily due to excitation and ionization of the sample.

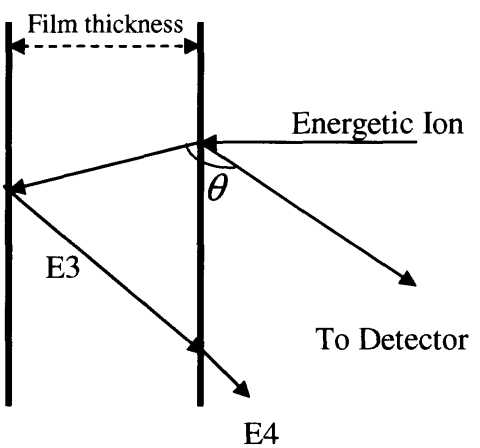


**Figure 4.5** Principle of Rutherford back scattering.

Energy of recoiling ions from nuclear collision depends upon on mass and energy. The number and energy of back-scattered incident ions gives us information about the film thickness, nature of the elements present [11]. Amount of back-scattered ions is proportional to concentration of that element. The ion beam generally of He element is used for the measurement. These energized ions enter the beam line of high vacuum and

then are focused. Magnets are used to disperse ions according to masses of the ions. The back-scattered ions are detected by the detector and electronic signals from these are amplified and plotted in terms of ions scattered back and voltage (energy).

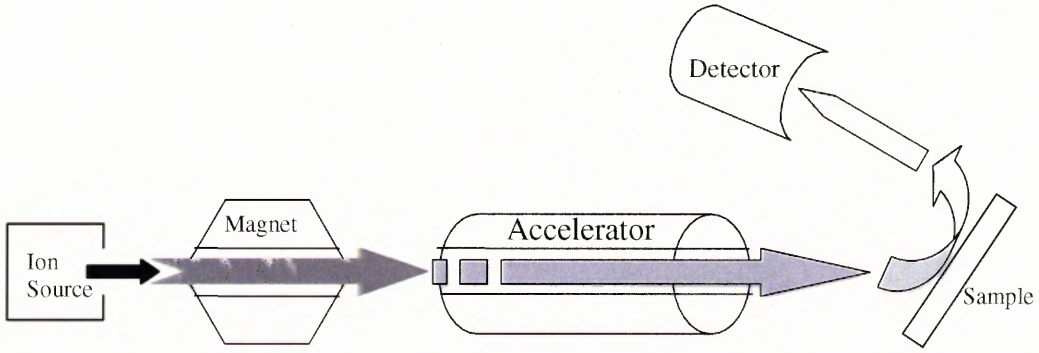


**Figure 4.6** Rutherford back scattering instrument [35].

The characterization for thin film thickness was carried out at Tandem Accelerator Laboratory, Rutgers University. Analysis was carried out using the Microsoft windows compatible software "SIMNRA". SIMNRA is explained in detail in the appendix.

# CHAPTER 5

# EXPERIMENTAL RESULTS

This chapter presents results and analysis of series of experiments using the magnetron sputtering system supplied with RF Power with emphasis on the effect of substrate biasing.

## 5.1 Sputtering Source Operation

Prior to sputtering the process chamber was baked to remove moisture. The vacuum in the range of 1X $10^{-6}$ Torr was attained before carrying out the deposition. The process is started after argon gas is allowed to flow through the chamber. The flow was set at 18 sccm with mass flow controller. To ignite the plasma the gas pressure inside the chamber was increased initially to few hundred mtorr by partially closing the gate valve. The standard power used in this study for deposition was 150 W at 5 mT pressure.

As explained in previous sections, for impedance matching a manual RF tuning controller was incorporated. There were two tuning controller settings under which the RF system was operated. First setting was at M1 = 7.5 V, M2 = 5 V (showing relative position of capacitors in terms of voltage) when reflected power ($P_{R)}$ observed was ~12-16 W. After gaining some experience with the tuning a second setting was found at M1 = 7 V, M2 = 6V when reflected power ($P_R$) observed was ~2 W at the forward power $P_F$ = 150 W. The power delivered to the source $P_S = (P_F - P_R)$.

The tuning did not require readjustment for each set of experiments. The system operated smoothly and reliably. The only sparking was observed occasionally in plasma near the substrate holder insulators at biasing voltage near 400 V and above.

It was observed that DC voltage was developed on the target when supplied with RF power, which was measured by a meter on RF tuning controller. The instrument was calibrated and it showed that 500 V is equivalent to 0.2 mA** on the meter scale. Development of voltage on source also called "self bias" implies that RF sputtering was working well with the adopted tuning network.

The matching network adjusted for the minimum reflected power with the source power operating at supply power of 150 W was subsequently measured without changing the tuning set up using vector network analyzer. The input impedance of the matching network was calibrated for 50 Ω impedance at the network input. The matching network output impedance was measured to be Z = 7.5 Ω – j33.15 Ω under these given conditions. The impedance of the matching network transfer function was found at 12.04 MHz rather than at 13.56MHz used in the sputtering process. The difference may be due to non-linearity in the vector network analyzer operating at a very low power (~1mW) whereas the sputtering source operates at 150 W and above. The results of the matching network are attached in Appendix C. It can be concluded from that this is the impedance of the operating sputtering source.

### 5.2 Substrate Bias and Ion Current.

Experiments were carried out to find the effect of substrate bias ($V_B$) on substrate current ($I_S$) using RF sputtering. Current was read by ammeter connected between the substrate probe and ground (zero biasing) or between the substrate and the biasing voltage power supply; this arrangement is shown in figure 3.1. The substrate floating voltage ($V_f$) was measured with the ammeter disconnected.

### 5.2.1 Effect of RF with Substrate Bias

First series of experiments were carried to find out the effect of pressure on substrate current $I_S$ (ion current).

**Table 5.1** Effect of changing pressure on $I_S$ at $P_S$ = 189 W with zero biasing

| Pressure (mT) | $V_f$ (V) | Is (mA) |
|---|---|---|
| 2.8 | -- | 12 |
| 3 | -- | 12 |
| 5 | 10.02 | 10 |
| 10 | 9.42 | 9.3 |
| 20 | 8.42 | 8.6 |
| 40 | 8.2 | 7.4 |

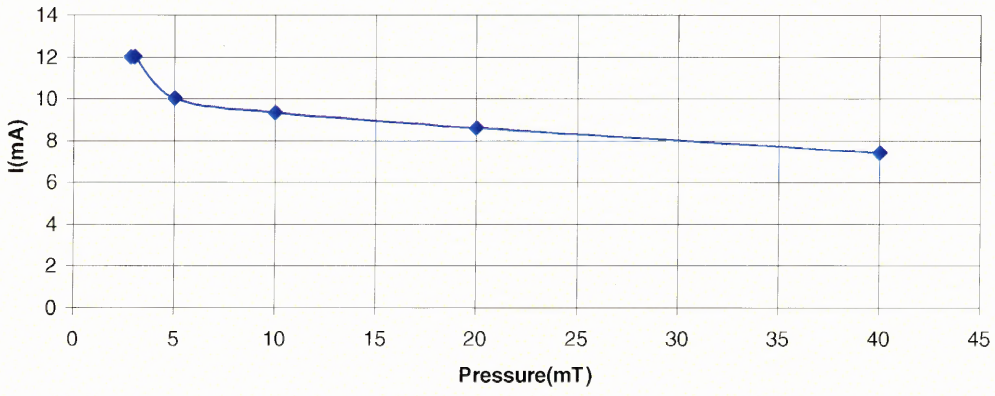


**Figure 5.1.A** Dependence of Is on pressure at Ps = 189 W with zero biasing.

** It is recommended to change a resistor in the meter so as to use the full range of the meter for the dc voltage developed on the sputtering target.

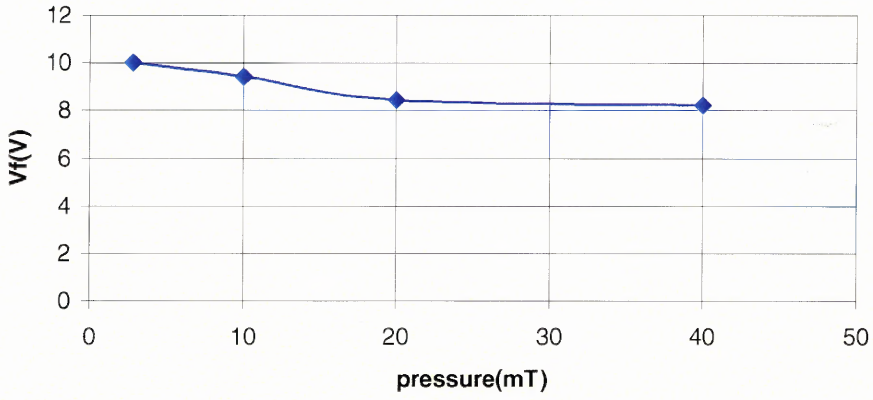


**Figure 5.1.B** Dependence of $V_f$ (V) on changing pressure (mT).

**Table 5.2** Effect of pressure on $I_S$ at $V_B$ = - 100 V and $P_S$ = 190 W

| Pressure (mT) | Is (mA) |
|---|---|
| 5 | 14.5 |
| 10 | 14 |
| 20 | 11.5 |
| 30 | 10.2 |

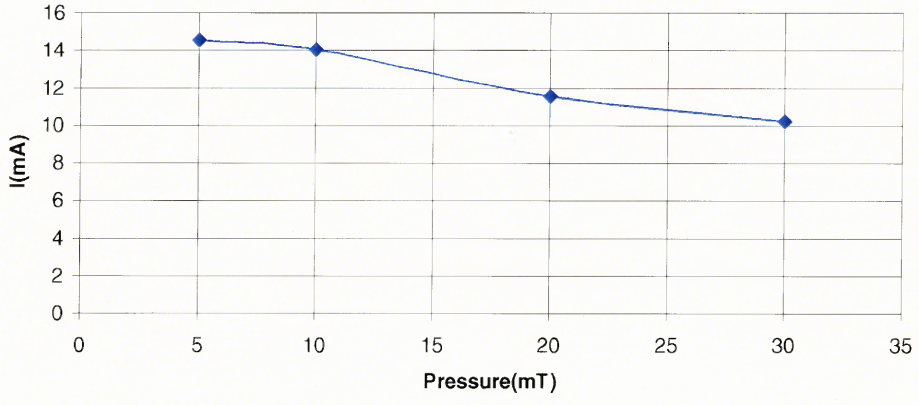


**Figure 5.2** Effect of pressure on $I_S$ at $V_B$ = - 100 Volts, $P_S$ = 190W.

**Table 5.3** Effect of $V_B$ (V) on $I_S$ (mA) at pressure of 8.4mT (188W), 2.8mT (178W), 5mT (138W)

| $V_b$ (V) | Is (mA) at 2.8mT Ps = 178W | Is (mA) at 5mT Ps = 138 W | Is(mA) at 8.4mT Ps = 188W |
|---|---|---|---|
| 0 | -- | 10 | 11 |
| -10 | -- | 11 | -- |
| -65 | -- | -- | 13 |
| -100 | 14 | 12 | 13 |
| -200 | -- | 12.5 | -- |
| -206 | 14.2 | -- | -- |
| - 240 | -- | -- | 14 |
| -300 | 15 | -- | -- |
| -400 | 15.5 | -- | -- |
| -500 | 15.7 | -- | -- |

The current at positive bias voltage $V_B$ = 4 V was 9.5 mA and at $V_B$ = 2 V was 10.1 mA for pressure 8.4mT.

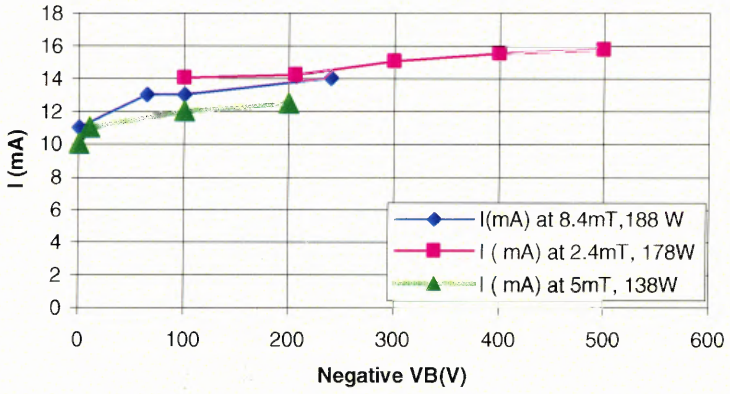


**Figure 5.3** Dependence of $I_S$ on $V_B$ at pressure of 8.4mT (188W), 2.8mT (178W), 5mT ($P_S$ = 138W).

This experiment was part of the series to find effect of substrate biasing on ion current. It was repeated with the source shutter closed to find the ion current contributed

by the other side of the substrate holder, which is not directly subjected to the source. Floating voltage $V_f$ observed was 12.10 V and current 14 mA for zero biasing with the shutter open.

**Table 5.4** Effect of $V_B$(V) on $I_S$ ( mA) with $P_S$ = 148 W

| $V_B$ (V) | $I_S$ (mA) | I shutter closed (mA) |
|---|---|---|
| 0 | 14 | 0.40 |
| - 150 | 15 | 0.50 |
| - 200 | 15.5 | 0.55 |
| -300 | 16 | 0.6 |
| -400 | 17 | 0.7 |

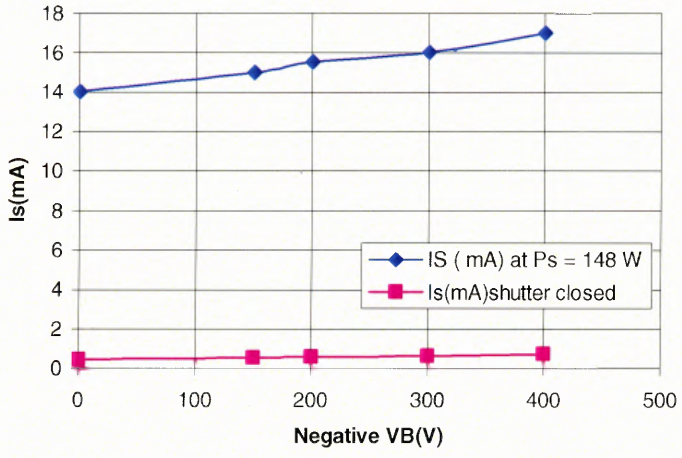


**Figure 5.4** Effect of $V_B$ (V) on $I_S$ (mA) on other side of substrate holder.

Ion current contributed from other side of the substrate holder with shutter closed (lower plasma density) was observed as 3-5 % of the total ion current.

Another series of experiment was carried to investigate the effect of varying RF power ($P_F$) on the substrate current ($I_S$) and the floating voltage $V_f$(V). This experiment was carried at pressure of 5mTorr

**Table 5.5** Effect of $P_F$ on $I_S$ and $V_f$ at zero biasing and operating pressure of 5 mTorr

| $P_F$(W) | $I_S$(mA) | **$V_F$(V) |
|---|---|---|
| 150 | 10 | 11.04 |
| 200 | 13 | 11.13 |
| 300 | 18 | 12.64 |
| 400 | 22.5 | 14 |
| 500 | 26 | 15.11 |
| 600 | 29.5 | 15.53 |

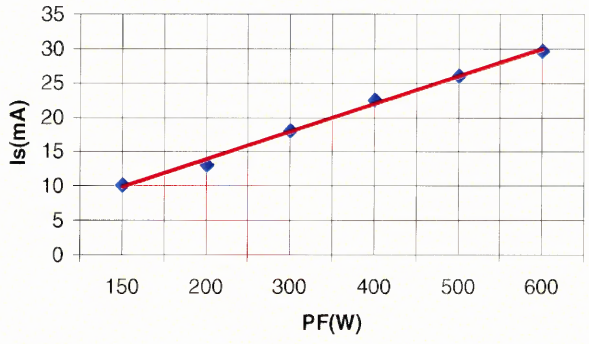


**Figure 5.5.A** Effect of $P_F$ on $I_S$ at zero biasing and operating pressure of 5 mTorr. The line shows linear fit to the data.

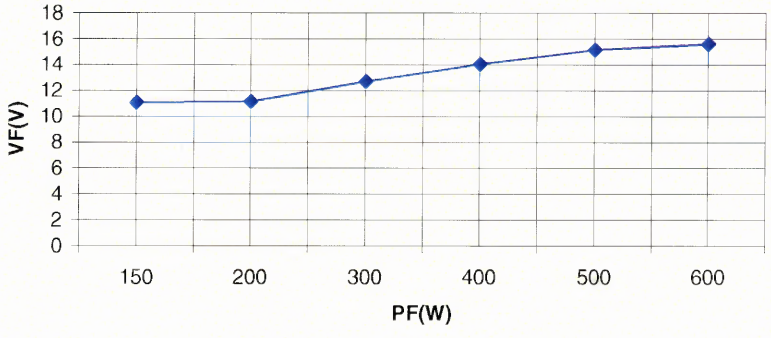


**Figure 5.5.B** Effect of $P_F$ on $V_f$ at operating pressure of 5mTorr.

It is observed that with increase in RF power there is proportional increase in substrate current $I_S$ (mA). The trend line y = 4.029x + 5.73 is shown in Fig. 5.5A.$V_f$ also increases due to higher ionization.

### 5.2.2 Comparison of Ion Current of DC Sputtering

Experiments were carried out to investigate the effect of substrate biasing ($V_B$) with DC sputtering on substrate current ($I_S$). The experiments were carried out at constant source current of 0.5 A for 350V and 1 A for 410V at operating pressure of 5 mTorr.

Table 5.6 presents the data of substrate current ($I_S$) with biasing voltage $V_B$ (V) for the two conditions of DC magnetron source operation. The data are presented graphically in figure 5.6

**Table 5.6** Effect of $V_B$(V) on $I_S$ with DC sputtering for $V_S$ = 350 V (0.5 A) and 410 V (1A)

| $V_B$ (V) | $I_S$ (mA) at 350 V and 0.5A | $I_S$ (mA) at 410 V and 1A |
|---|---|---|
| 0 | 0.108 | 0.533 |
| 10 | 1.2 | -- |
| 11 | -- | 7.72 |
| 20 | 1.3 | -- |
| 21 | -- | 7.95 |
| 30 | 1.32 | 8 |
| 50 | 2.1 | 8.1 |
| 70 | 2.14 | 8.16 |
| 100 | 2.19 | 8.24 |
| 130 | 2.24 | 8.3 |
| 150 | 2.27 | 8.37 |
| 180 | 2.3 | 8.44 |
| 200 | -- | 8.44 |
| 207 | 2.34 | -- |
| 250 | 2.39 | 8.58 |
| 300 | 2.45 | 8.68 |
| 350 | 2.51 | 8.79 |
| 400 | 2.58 | 8.89 |

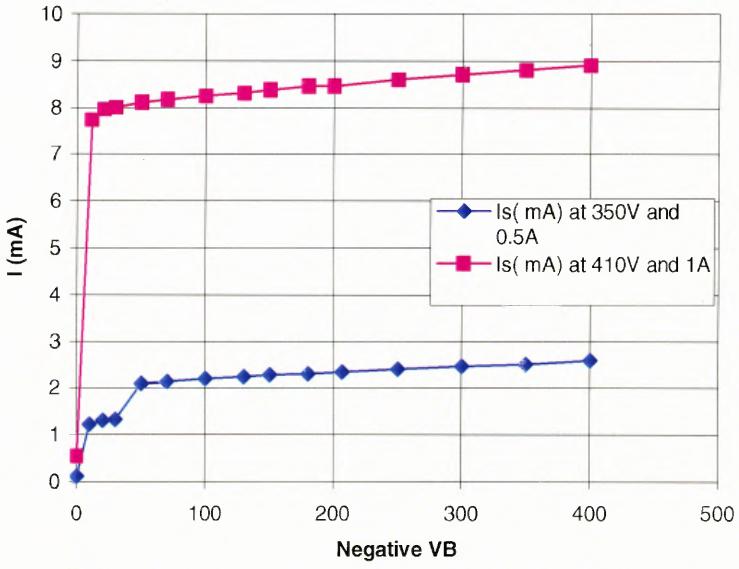


**Figure 5.6** Dependence of $I_S$ on $V_B$ for DC sputtering at Vs of 350 V (0.5 A) and 410 V (1A).

For DC sputtering $V_F$ (V) of 0.23 V was observed when target was at 350 V (0.5A) where as $V_f$ (V) of 0.91V was observed for target at 410 V (1A). For comparison of $I_s$ and its dependence on bias voltage $V_s$ for RF sputtering is shown in Table 5.7, below.

**Table 5.7** Effect of $V_B$ (V) on $I_S$(mA) at two different RF tuning conditions at 5mT

| $V_B$ (V) | $I_S$ (mA) at $P_S$ = 148w | $I_S$ (mA) at $P_S$ = 138w |
|---|---|---|
| 0 | 12.5 | 10 |
| -10 | -- | 11 |
| - 100 | 14 | 12 |
| - 200 | 15 | 12.5 |
| - 300 | 15.5 | -- |
| - 400 | 16 | -- |

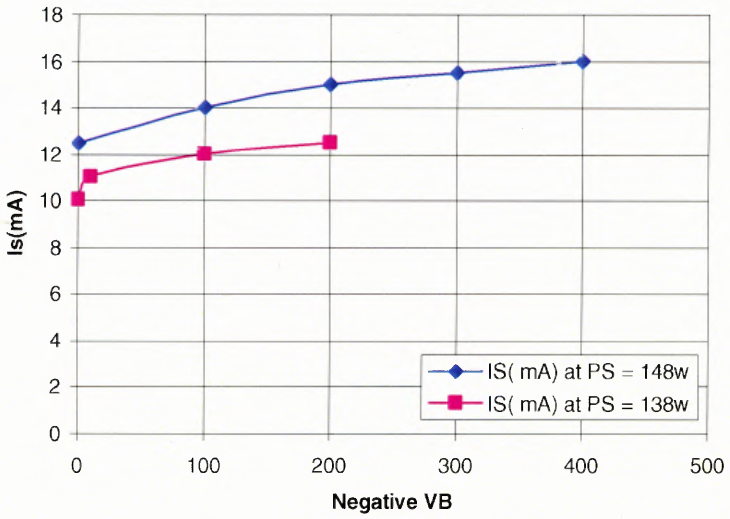


**Figure 5.7** Effect of $V_B$ (V) on $I_S$(mA) at two different RF tuning conditions.

It was observed that with better tuning, ie less reflected power $P_R$ for source power of 150 W, the substrate current ($I_S$) increased approximately by 20 %.

On making the comparison between the two conditions of DC magnetron source operation with biasing, it was observed that ion current increases dramatically with increase in source power. There is a rapid initial increase of $I_S$ with biasing voltage but the substrate current then slowly with increase in bias, as is graphically represented in Figure 5.6. On comparing the substrate current at two different RF powers similar trends were observed except that ion current is higher in case of RF as compared to DC. Also the substrate current is high at zero bias in the RF case.

### 5.2.3 Temperature of Substrate during RF Sputtering with DC Biasing

This experiment was conducted to find if there was any temperature increase of the substrate due to biasing. Temperature is an important parameter, which can lead to crystallographic phase change of tantalum. For this experiment a new substrate holder

from thin aluminum sheet (thickness 0.018") was used. A thermocouple was attached at the center of the holder to measure the temperature. Power of $P_S$ = 148W was supplied to the target. Thin aluminum holder was put to bias voltage ($V_B$) of -200V, substrate current $I_S$ of 13 mA was observed, with initial temperature 25 $^0$ C and final stabilized temperature reached was 151 $^0$ C in 10 minutes. Another experiment was carried out using the standard thick stainless steel holder explained in section 3.1 with a thermocouple attached to its backside. Temperature readings were taken in 10 minutes steps after opening the shutter above the source operating with the same parameters as for thin aluminum sheet. The results are shown in table 5.8.

**Table 5.8** Temperature variation of thick stainless steel holder

| Time (minutes) | Initial Temperature ° C | Final Temperature ° C | Temp difference ° C |
|---|---|---|---|
| 10 | 25 | 64 | 39 |
| 20 | 64 | 92 | 28 |
| 30 | 92 | 111 | 19 |
| 40 | 110 | 123 | 13 |

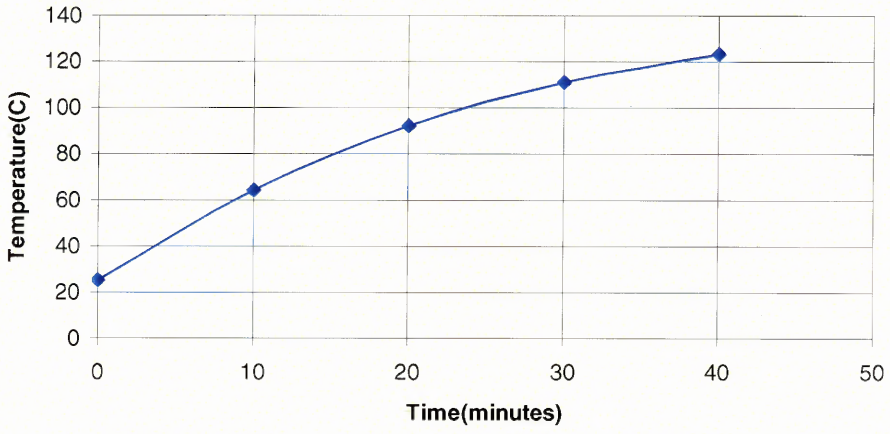


**Figure 5.8** Temperature (° C) variations with time (minutes) for thick substrate holder.

Both measurements show that the substrate temperature does not reach the critical value (400°C) that affects the phase of the tantalum films [9]

### 5.3 Effect of Substrate Bias on Crystallographic Phase of Ta Film

X- ray diffraction was used to analyze crystallographic phases of samples of Ta films deposited by RF magnetron sputtering with different substrate biasing. XRD technique is described in chapter 4.1. Table 5.9 and 5.10 show the ratio of β/α phase defined as the ratio of the counts per minute registered by an XRD counter at the maxima of Ta β phase for (002), (004) peaks around 2θ angle of 33.56° and 70.52 respectively while Ta α phase (110), (220) peaks are observed near 2θ angle of 38.44° and 70.52° respectively.

**Table 5.9** XRD analysis for Silicon samples at different biasing conditions

| Sample # | Substrate Type | Biasing Voltage (V) | XRD Results | β/α |
|---|---|---|---|---|
| Pta 7o | Silicon | 0 | 002(β), | All β |
| Pta 6o | Silicon | - 100 | 002(β), 110(α) | 2.5 |
| Pta 5o | Silicon | - 200 | 110(α), 220(α) | All α |
| PTa 2o | Silicon | 0 | 002(β) | All β |
| PTa 1o | Silicon | -150 | 002(β), 004(β) | 27.5 |
| PTa B o | Silicon | - 200 | 110(α), 220(α) | All α |
| PTa 7 o | Silicon | - 300 | 002(β) 004(β) | All β |
| PTa 6 o | Silicon | - 400 | -- | -- |

**Table 5.10** XRD analysis for Aluminum samples at different biasing conditions

| Sample # | Substrate Type | $V_B$ (V) | XRD Results | β/α |
|---|---|---|---|---|
| PTa 7Al | Aluminum | 0 | 002(β), 110(α), 220 (α), 004 (β) | 0.149 |
| PTa 6 Al | Aluminum | - 100 | 002(β), 110(α), 220(α) | 0.2 |
| PTa 5 Al | Aluminum | - 200 | 110(α), 220(α) | All α |
| PTa 2 Al | Aluminum | 0 | 002(β), 110(α), 004 (β) | 2.6 |
| PTa 1 Al | Aluminum | - 150 | 002(β), 110(α), 004 (β) | 0.1162 |
| PTa B Al | Aluminum | - 200 | 110(α) | All α |
| PTa 7 Al | Aluminum | - 300 | 110(α) | All α |
| PTa 6 Al | Aluminum | - 400 | 110(α) | All α |

The XRD patterns of representative samples are shown in Fig. 5.9 for Si substrate and in Fig. 5.10 for Al substrate. The consistent results of XRD showed that substrate bias promotes the generation of α phase on aluminum and silicon though on aluminum it is more pronounced as compared to silicon. It was observed that in case of Silicon it changes to α phase at -200 V biasing whereas it reverts back to β at -300 V biasing.

No satisfactory XRD data was obtained on Silicon at biasing voltage of -500 V. Either no or very negligible signal was received for these samples. Samples were analyzed for film thickness and it was observed that film thickness decreases with higher substrate biasing voltage. This data of XRD analysis is presented in tables 5.9 and 5.10 for silicon and aluminum respectively.

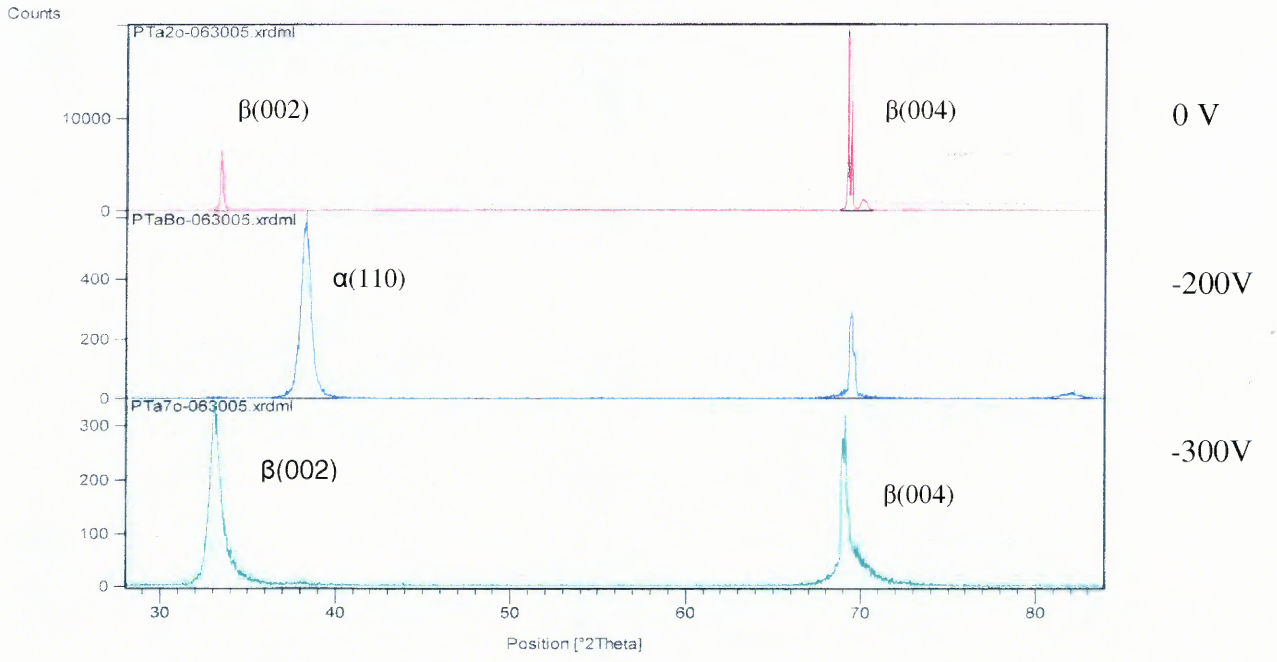


**Figure 5.9** XRD results for Ta films on Si substrate at different voltage biasing conditions shown in table 5.9.

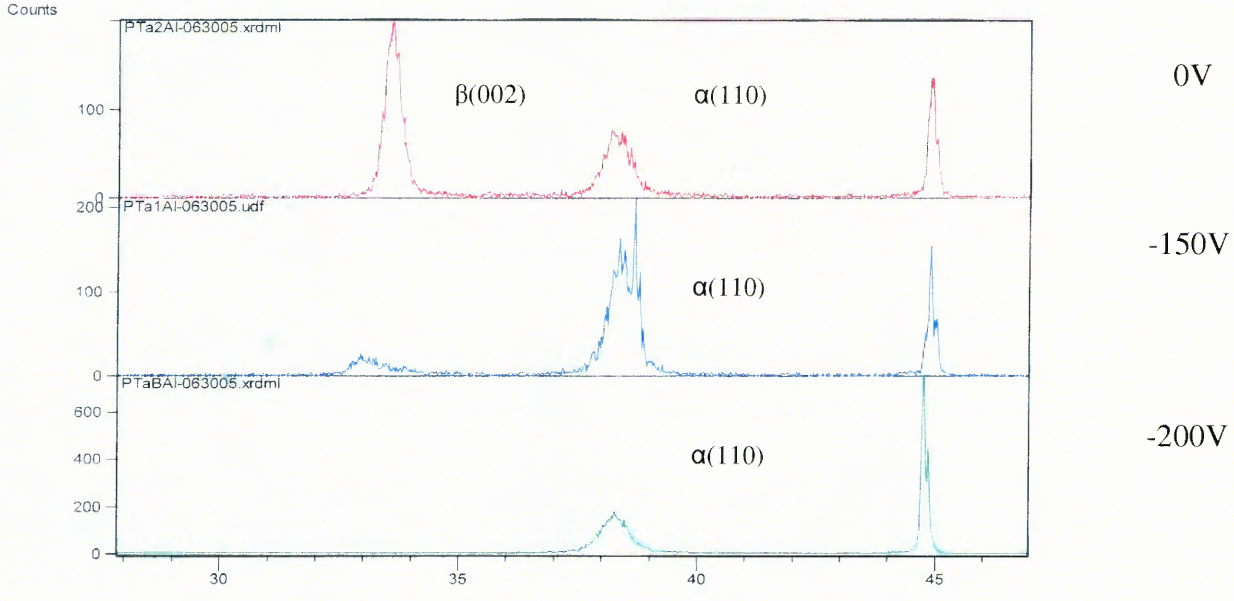


**Figure 5.10.A** XRD results for Ta films on Al substrates at different biasing voltage.

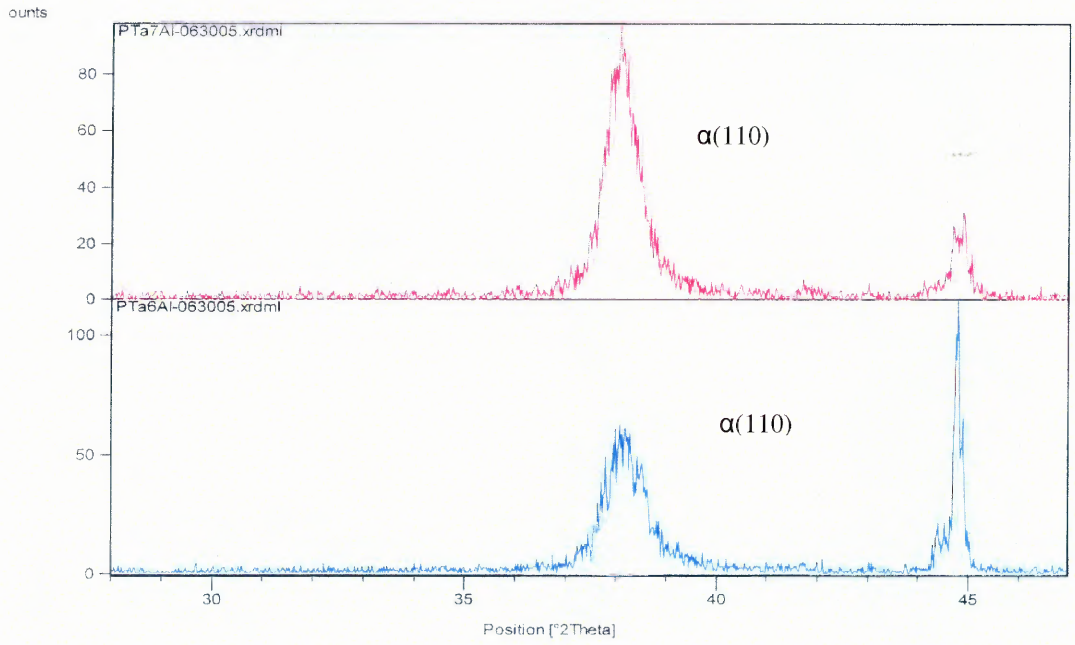


**Figure 5.10.B** XRD results for Ta films on Al substrates at different biasing voltage.

### 5.4 Effect of Substrate Bias on Thickness of Ta Films

RBS technique was used to measure the film thickness. The ion used for the bombardment is $^{4}He_{2}$ with energy of 2000keV.The principle and process of this characterization technique is explained in chapter 4.2. The area under a spectral peak represents the total number of atoms of a given element present within a layer. Peak height is directly proportional to the atomic concentration. The peak width (ΔE) depends on the maximum length traversed by the incoming projectile ions in the layer, or to the layer film thickness.

The simulations were carried out by the windows compatible program SIMNRA. Calibration offset and energy per channel are set at 35.5 keV and 6.64 keV respectively. The fit of Ta simulated spectra to the actual was done by changing the number of Ta atoms/ $cm^2$. The total number of ions bombarding the sample was adjusted to make the

Ta peak height same as simulated spectra. Examples of RBS data and corresponding simulations are shown in figures 5.11.A, 5.11.B, and 5.11.C. The results of derived film thickness are summarized in table 5.11 Thickness in nm and deposition rate in nm/s was calculated from the atomic surface density using the bulk Ta density of 16.6 g/cm$^3$. The RBS spectra for films on glass and aluminum substrates are attached in appendix B, C, and D

The results clearly indicate that thinner films are deposited at higher substrate bias voltage. RBS spectra show a prominent peak of Ta and a distinct age of Si substrate. In the data of films deposited with high substrate bias voltage a characteristic broad peak in the intermediate position (between Si and Ta) is seen. Simulations indicate that it may be due to incorporation of Ar in the film Figure 5.11.A, 5.11.B and 5.11.C. Ar concentration as high as 14% is indicated by simulation for the film deposited with -400 V bias shown in Figure 5.11.E

**Table 5.11** Substrate type, $V_B$, thickness of film, deposition rate, atoms/ cm$^2$

| Substrate Type | Biasing Voltage (V) | Atoms/ cm$^2$ | Thickness (nm) | Deposition Rate (nm/sec) |
|---|---|---|---|---|
| Silicon | 0 | 1.42 E 18 | 255 | 0.425 |
| Silicon | -300 | 6.90 E 17 | 124 | 0.206 |
| Silicon | -400 | 5.65 E 17 | 102 | 0.170 |
| Glass | 0 | 1.55 E 18 | 281 | 0.468 |
| Glass | -200 | 5.75 E 17 | 103 | 0.171 |
| Aluminum | -400 | 6.70 E 17 | 121 | 0.201 |

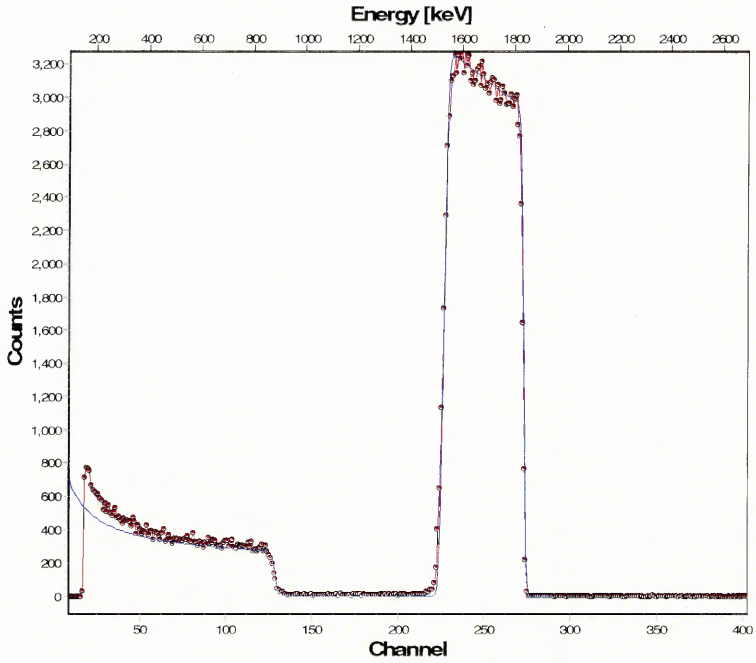


Figure 5.11 A shows Ta peaks at zero biasing.
Red line:desired
Blue line:Simulated

**Figure 5.11.A** RBS for Si (100) at zero biasing showing peaks of Ta.

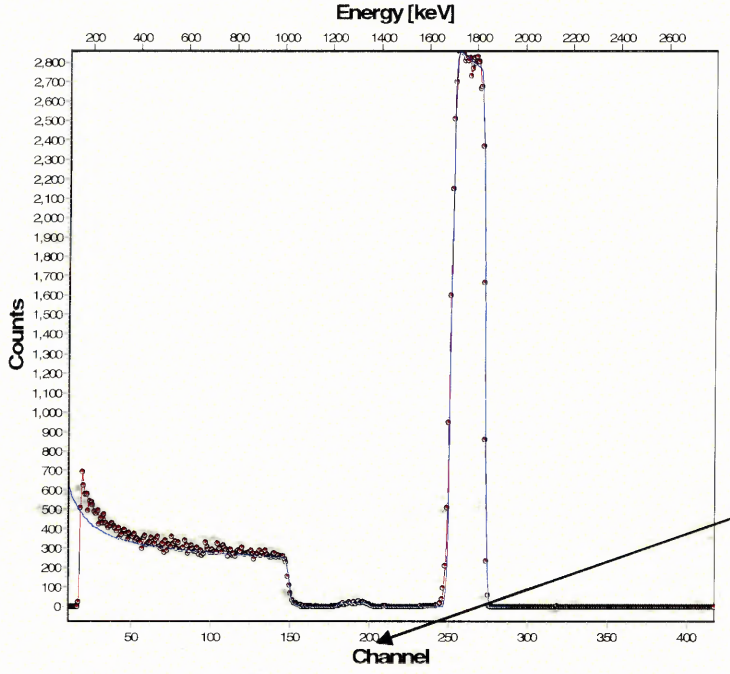


Figure 5.11B shows Ta peak at -300V biasing
Red line:desired
Blue line:Simulated

**Figure 5.11.B** RBS spectra for Ta film on Si (100) at -300V biasing.

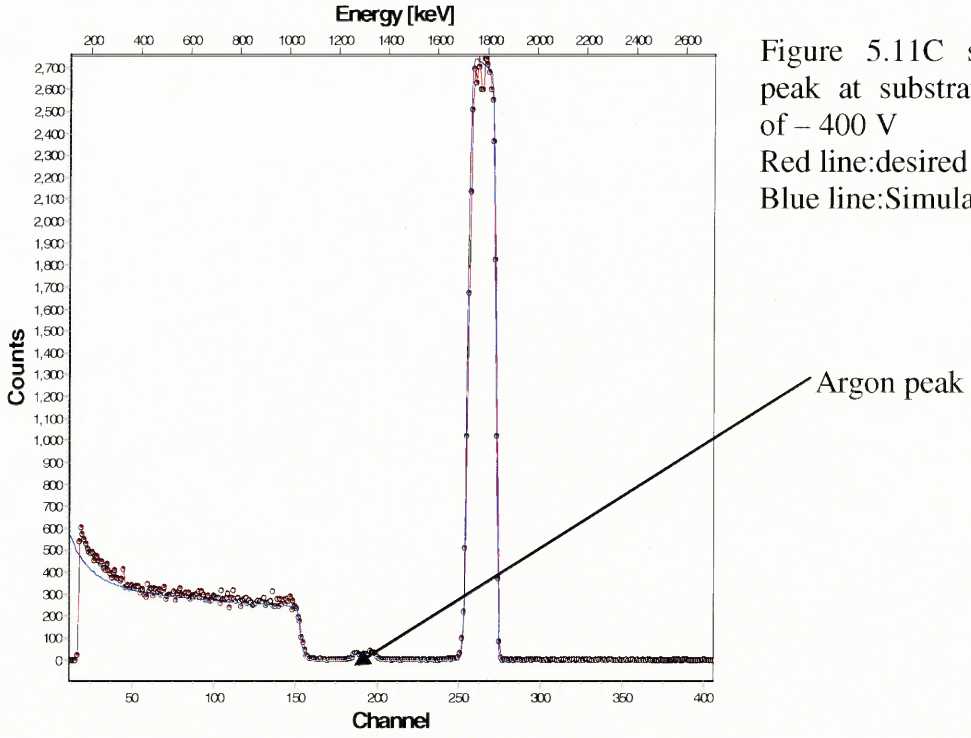


Figure 5.11C shows Ta peak at substrate biasing of – 400 V
Red line:desired
Blue line:Simulated

**Figure 5.11.C** RBS for Si(100) at -400V biasing showing peaks of Ta and Argon.

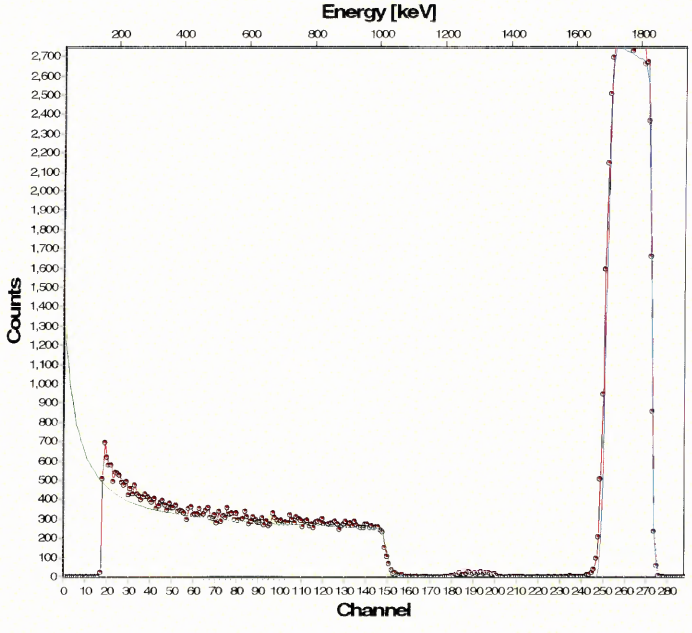


Figure 5.11.D shows the peaks for Ta, Ar and Si
Red: Acquired Simulation for Ta from RBS
Blue: Simulated for Ta
Green: Simulation for Si
Purple: Argon
It contains 10% of Argon.

**Figure 5.11.D** RBS for Si(100) at -300V biasing showing peaks of Ta Si, and Argon.

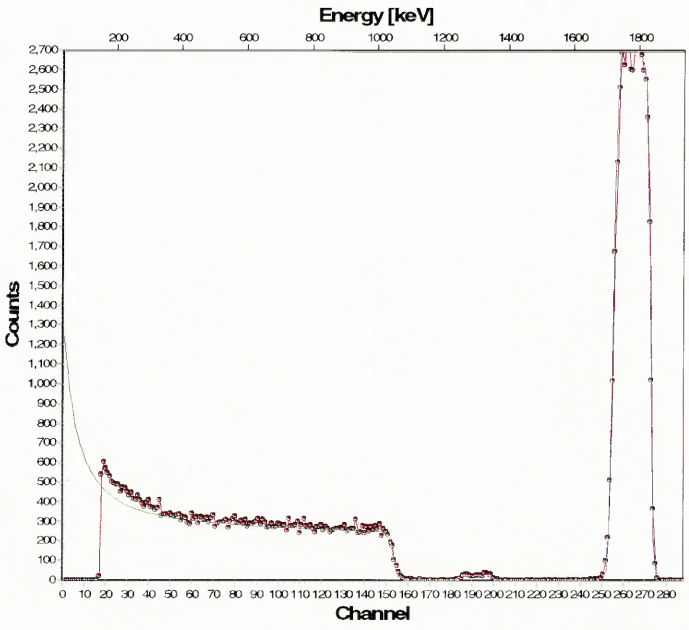


Figure 5.11.D shows the peaks for Ta, Ar and Si
Red: Acquired Simulation for Ta from RBS
Blue: Simulated for Ta
Green: Simulation for Si
Purple: Argon
It contains 14% of Argon

**Figure 5.11.E** RBS for Si(100) at -400V biasing showing peaks of Ta Si, and Argon.

# CHAPTER 6

# DISCUSSION AND ANALYSIS

This chapter discusses and analyzes the experimental and characterization results of Ta thin films. The effect of RF sputtering and substrate DC bias on Ta films is investigated.

The first big challenge for carrying out this study was to match the impedance of the magnetron source to that of RF generator to generate plasma. This problem was solved by adopting a matching network and constructing a tuning controller for it. Experiments were carried to study effect of biasing voltage or ion bombardment on the film growth on different substrates like Al, $SiO_2$/ Si, Steel and glass.

## 6.1 RF Sputtering Operation

RF sputtering was carried out using RF generator, which is connected to the magnetron sputtering source in the chamber through a co-axial cable and a matching network. The system is explained in detail in section 3.2, and its operation in section 5.1. The impedance matching between the source and RF generator is achieved by manual tuning of capacitors of the matching network. Tuning is done by monitoring the amount of reflected power, which was as low as ~ 2W at the forward power of 150 W. Depositions were carried at gas pressure of 5mTorr.

Plasma, a necessary condition for sputtering, is a partially ionized gas in which free electrons collide with neutral atoms resulting in generation of species like ions, electrons and photons. At a high frequency of 13.56MHz, electrons have high energy of order of few hundred eV, which facilitates ionization of gas. The ions on the other hand are heavier and are not much accelerated by the rapidly oscillating electric field and their

energy is in the range of few hundredth of an eV (~ 0.01 eV) [30]. Since electrons have higher velocity, their flux on any surface in contact with plasma, including the chamber wall, is higher than the flux of ions. This loss of electrons makes plasma positive, with respect to its container, usually at ground. The resulting electric potential at the edge of plasma limits the loss of electrons and facilitates the flux of ions. For an isolated object in plasma both fluxes are the same, resulting in zero current.

An electrically floating surface placed in plasma develops potential called as floating potential. This potential developed on the floating surface is dependent upon electron temperature and electron – ion density. The temperature is lower near the floating surface due to lower energy of electrons, so Vf is lower than the plasma potential. The net potential is given by (Vp – Vf), since the other electrode is grounded. This is shown in Figure 6.1.

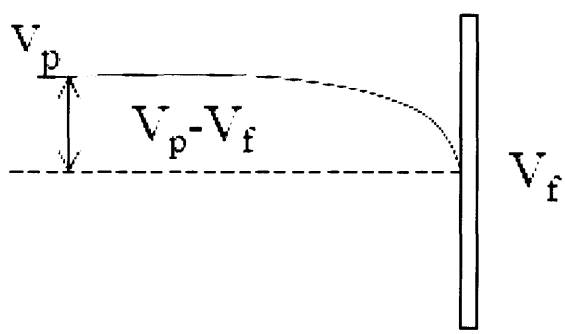


**Figure 6.1** Floating substrate at lower potential than plasma potential.

This potential on the surface called floating potential is given by the equation [14]

$$Vf = -\frac{kTe}{2e} \times \ln\left(\frac{m_i}{2 \times \pi \times m_e}\right) \qquad (6.1)$$

Here
$m_e$ = mass of electron
$m_i$ = mass of ion
Te = electron temperature

The floating potential is measured by the setup, as shown in the Figure 6.2

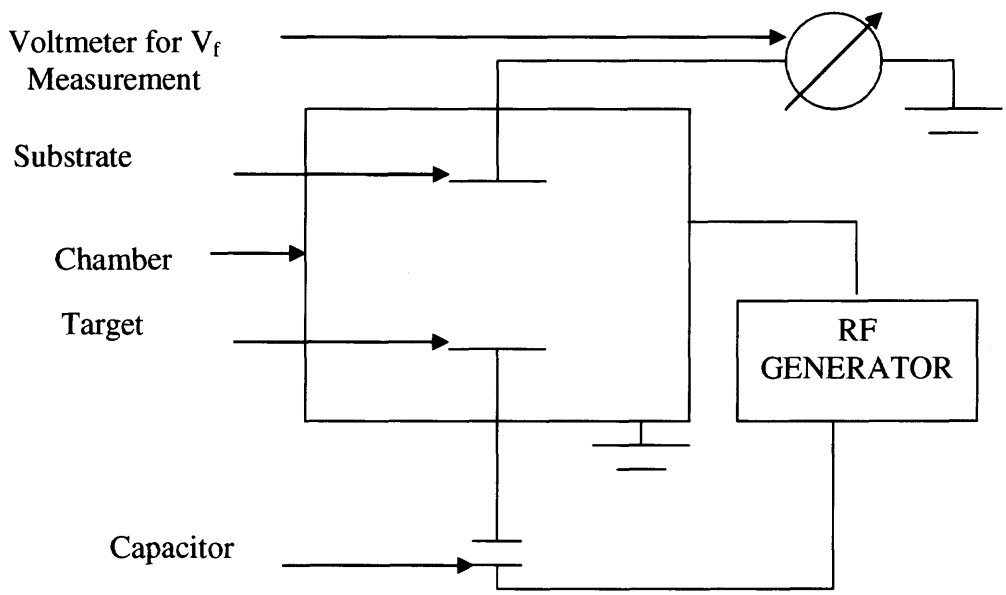


**Figure 6.2** Schematic of the substrate floating voltage measurement circuit.

The power applied to the target electrode is through a coupling capacitor. If electrodes are equal then potential developed on both the electrodes is equal because DC Voltage developed depends upon the area and is given by equation 6.2 [14]

$$V_1/ V_2 = (A_2/ A_1)^n \qquad (6.2)$$

$$n \sim 4$$

DC voltage developed is the voltage drop between the plasma and electrode 2. Equation 6.2 is valid for the electrode, which is powered. If electrode1 and electrode2 is grounded then DC voltage is the potential of plasma.

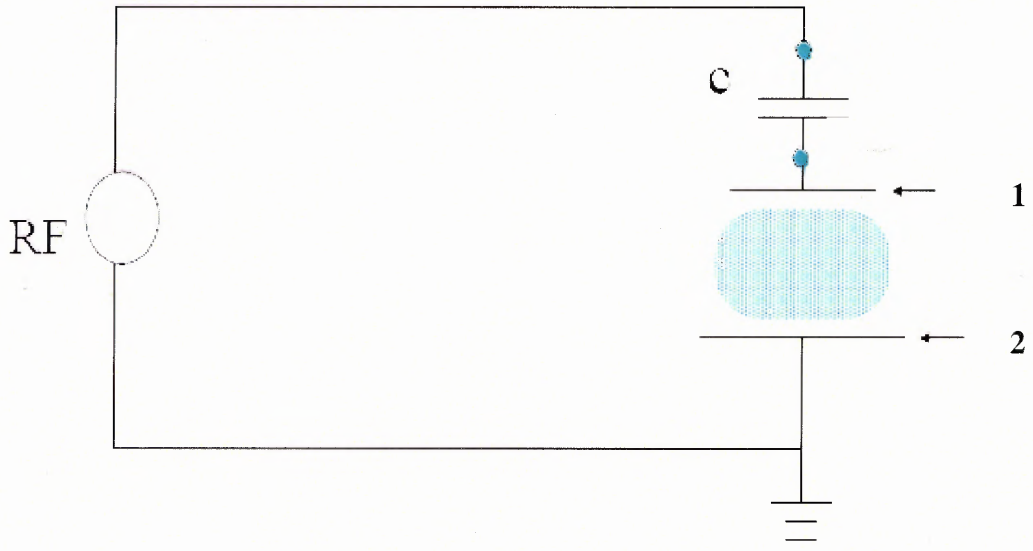


**Figure 6.3** Schematic of high frequency glow discharge circuit [14].

Figure 6.4 shows the voltage distribution in the RF powered glow discharge. It also shows development of DC voltage on unequal and electrodes.

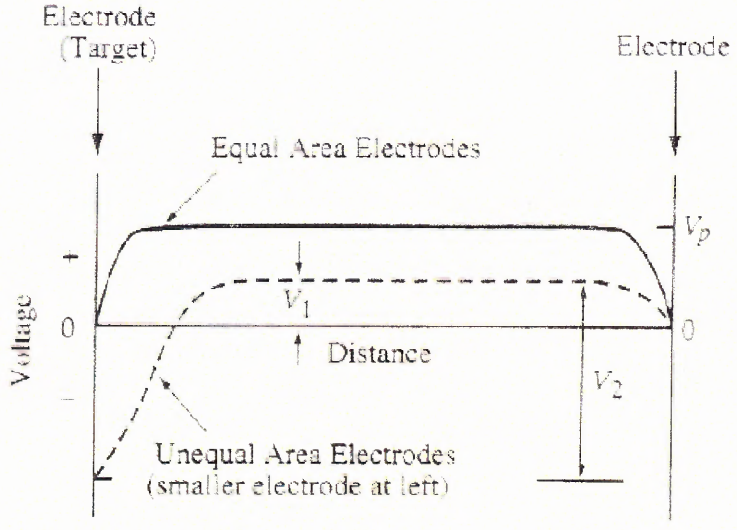


**Figure 6.4** Average voltage distributions in RF powered glow discharge [30].

The smaller electrode has larger sheath and higher potential therefore producing more ion bombardment so it will be bombarded with ions continuously. This leads to development of potential called DC self bias. DC voltages depend on RF power, gas and

gas flow, pressure of gas, geometry of the chamber. Experiment was conducted and this negative DC self bias was viewed on oscilloscope. The amplitude of the sine wave was 200 V and time period of the cycle was 7.4 X10 $^{-8}$ sec.

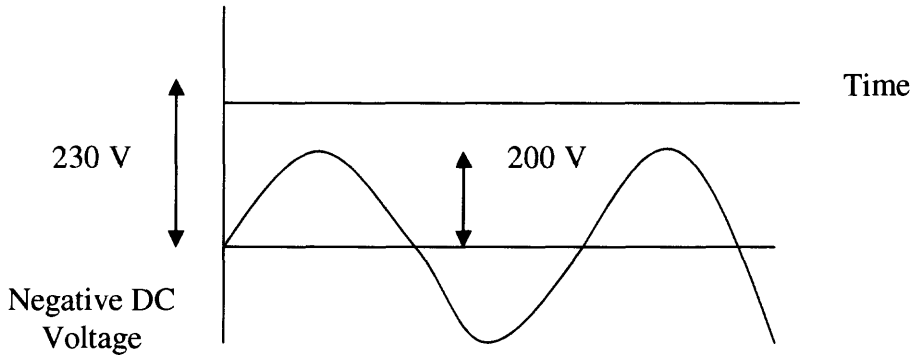


**Figure 6.5** Superimposed RF voltages on negative DC bias voltage on target.

## 6.2 Substrate Bias and Ion Current

The aim of this study was to investigate the effect of RF sputtering with substrate bias on Ta film deposition because it was expected that ion bombardment may affect the film properties. Ion current on a biased substrate was observed in both DC and RF sputtering. In DC sputtering ion current was very small at zero bias (2.81 $\mu A/cm^2$ for supply voltage of 350V and 4.43 $\mu A/cm^2$ for 410V) but rapidly increased with increase in negative voltage biasing and saturated at $2mA/cm^2$ and $8mA/cm^2$ respectively. It was also observed that at higher target voltage ie 410 V the ion current increased approximately four times more than that at 350 V, while the source power increased ~ 4.5 times.

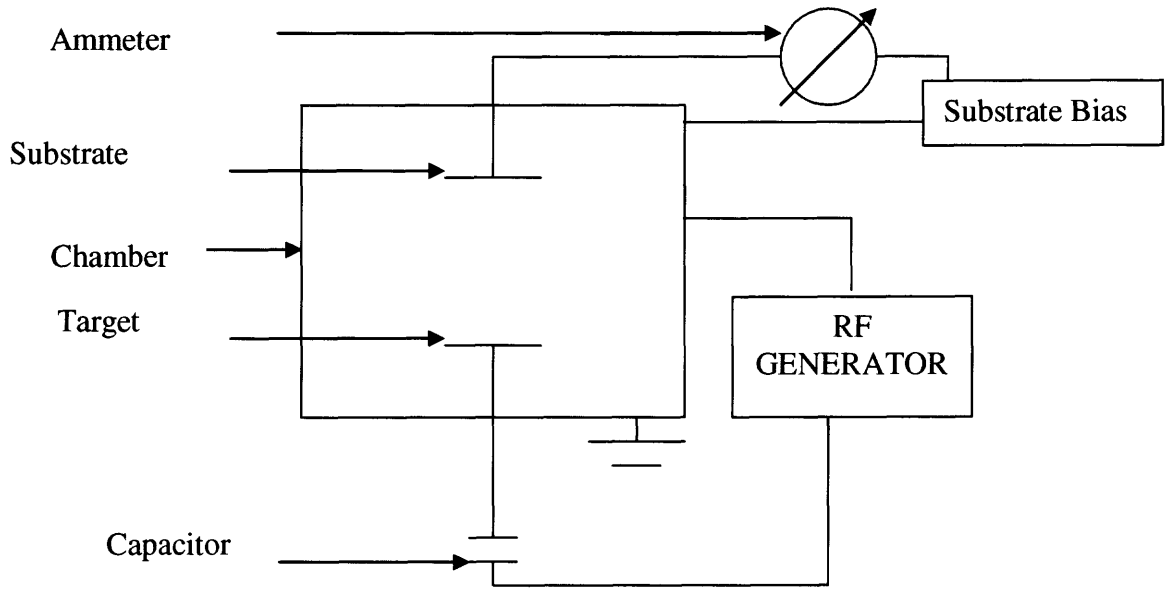


**Figure 6.6** Schematic of the substrate floating voltage measurement circuit.

With RF sputtering a high ion current (10 mA/cm$^2$) was observed even at zero bias and it increased moderately with increase in negative voltage biasing (17 mA/cm$^2$ at -400 V). The higher ion current with RF power shown in Figure 5.7, it can be explained by the fact that RF power at high frequency creates ionization inside the chamber. It was also observed that with increase in pressure ion current decreases as shown in Figure 5.1A, 5.2. This may be explained by the fact that as sputtering gas pressure increases, ionization decreases as number of electron – ion recombination outweighs the ionization of atoms due to decrease as the electron mean free path in plasma.

## 6.3 Effect of Substrate Biasing on Ta Films

This topic can be divided into two parts:

### 6.3.1 Film Thickness (re-sputtering)

RBS was used as a characterization technique to measure film thickness. It has been observed that at higher biasing voltages film thickness decreases and it is attributed to the fact that there is re-sputtering of the growing film by high-energy ions. "Sputtering yield is defined as average number of atoms (neutral or ions) ejected by an impact of an ion. It is dependent on energy of the primary ion, mass, incidence angle, and nature of sputtered material." [31]. Sputtering yield is also dependent on binding energy, and which depends upon the nature of material.

From the measured film thickness and the current of ions bombarding the substrate, the sputtering yield of Ta from the film may be estimated. The results of calculations for the films deposited on Si, for which RBS data were obtained, are shown in Table 6.1 The ion dose, defined as number of ions impinging the substrate, is calculated from the ion current and the substrate holder area from which ions are collected. The number of Sputtered atoms is the difference between the atoms/ $cm^2$ at zero biasing and atoms/ cm2 at biasing condition. While sputtering yield is defined as ratio of difference between atoms arriving at zero bias and atoms at different biasing to number of atoms arriving at zero bias.

While calculating these parameters some assumptions were made such as: number of atoms arriving at substrate is same whatever may be the biasing condition. These atoms get deposited and due to high energy of ions bombarding the substrate and are sputtered from the deposited film. It is assumed that at zero biasing sputtering of the

deposited film does not take place as the ions have energy near or below the sputtering threshold.

**Table 6.1** Sputtering yield, sputtered atoms, ions/deposited atom, ion dose of Ta film on silicon substrate

| Biasing Voltage ($V_B$) | $I_S$ (mA) | Ion Dose Ions/ $cm^2$ | Total number of deposited Atoms/ $cm^2$ | Ions/ Deposited Atom | Sputtered Atoms Atoms/ $cm^2$ | Sputtering Yield |
|---|---|---|---|---|---|---|
| 0 | 10 | 9.78 E 17 | 1.42 E 18 | 0.688 | 0 | 0 |
| -300 | 15 | 1.46 E 18 | 6.90 E 17 | 2.12 | 7.3 E 17 | 0.5 |
| -400 | 16 | 1.56 E 18 | 5.65 E 17 | 2.77 | 8.55 E 17 | 0.54 |

It is observed that Tantalum film thickness decreases with increase in bias voltage ($V_B$). The sputtering yield increases due to increase in ion dose and energy of ions.

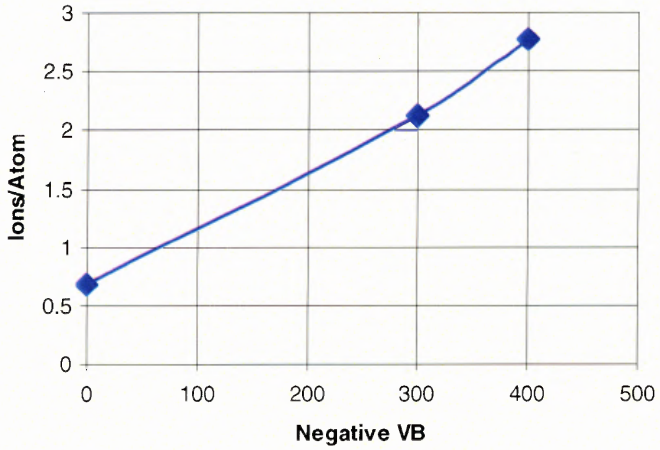


**Figure 6.7** Ratio of ions bombarding the substrate/ atom at different biasing conditions for Si.

### 6.3.2 Effect on Crystallographic Phase of Ta Films

XRD characterization technique was used for analysis of crystallographic phase in Ta films, deposited by RF sputtering with DC substrate bias. This XRD data in Figure 5.9, 5.10A, and 5.10B show significant and consistent influence of biasing on films deposited on silicon and aluminum substrates. Films on glass, $SiO_2$, and steel still need further investigation.

In the case of aluminum substrate, films with mixed phase were deposited with zero bias and with increasing voltage bias concentration of α phase in the Tantalum film increased from 0.149 (β/ α) to all α phase at -200V and above (table 5.10.A and Figure 5.10.B). The α phase Ta films on aluminum substrate have (110) orientation.

On Si substrates, β crystallographic phase was observed at zero biasing and α phase at -200V but β crystallographic phase appeared again at above -300 V. Growth of two different phases of Tantalum on different substrates at the same biasing condition for implies that the substrate also has an effect on the development and growth of different crystallographic phase.

The results show that crystallographic phase formation is dependent on energetic ion bombardment. Ion assisted deposition leads to removal of weakly bond atoms of the film and transfers high energy and momentum to the substrate atoms. Both effects, ie removal of weakly bonded atoms and high energy of atoms of substrate result in re-orientation and rearrangement of Tantalum crystal therefore change in phase of Tantalum.

The results in this study are different from other two studies [37], [38] reported in literature on Ta bias sputtering. According to reference [38] crystallographic phase of Ta

films on $SiO_2$ can be controlled by adjusting the impinging ion energy and ion flux (ratio of ion flux to Ta atom flux). For deposition of bcc Ta the energy was lower than 20 eV with ions to atoms flux ratio higher than 13. The instrument and the process conditions were different than those in the sputtering system used for this study (one DC and RF supply). The prior study was conducted using dual RF power supplies of frequency 42.4 and 13.56 MHz, and dual DC were used at gas pressure of 7mTorr. In the other prior study [37] on deposition Ta with substrate bias the processes were carried at lower gas pressure of 0.3 mT (4 X $10^{-2}$ Pa) at which processes were carried using dc magnetron sputtering source with substrate bias. Formation of bcc –Ta phase was observed at bias voltage below -100V. In contrast in the present study it was found that at higher bias voltage (-200V) induces formation of α phase on Al and Si substrate but under different process conditions than the two previous studies.

Sputtering yield depends on the target, ion mass and energy. For Ar ion impact on Ta the sputtering yield of 0.3, 0.6 and 1.0 were observed at 0.2keV, 0.6keV and 5keV [40]. The sputtering yield of 0.5 at 300eV and 0.54 at 400eV were observed in the present study.

The results of this study helped in finding conditions and parameters of RF sputtering with substrate bias, which resulted in deposition of α Tantalum phases on aluminum and silicon. Deposition of α Tantalum is an interest for applications such as in aluminum fuel cells, interconnects in semiconductor industry. This is achieved by standard RF magnetron condition with DC bias

# CHAPTER 7

## SUMMARY AND CONCLUSION

This research was aimed for understanding the process of RF sputtering with substrate biasing for deposition of Tantalum. A number of experiments were carried out to understand the effect of substrate biasing voltage, pressure, and RF power on the substrate ion current. The effect of ion current on Ta film deposited on different substrates such as silicon dioxide, silicon, aluminum, glass and steel were studied.

Comparison was made between substrate currents of DC sputtering and RF sputtering with DC bias. It was observed that using RF sputtering instead of DC sputtering resulted in subsequent increase in substrate ion current. The amount of ion current in RF sputtering was much higher at zero bias (10- 11 mA) than in DC sputtering (108-176μA) at zero biasing. Ion current increased with increase in substrate bias voltage and source power in both cases reaching 2.58 mA in DC sputtering at 175W power and 16 mA in RF sputtering at 148W power, with biasing voltage at - 400 V. Moreover, the ratio of Ta atoms to ions arriving at the substrate was much higher in RF case as the deposition rate for DC sputtering is approximately 3 times larger for the same source power.

Substrate biasing affected the crystallographic phase of thin films deposited by RF sputtering on Si and Al substrates. Only β phase was detected by XRD in films deposited on Si with zero bias voltage, similarly to the previous study with DC sputtering at room temperature [9]. Mixed composition of α and β phases were observed in films deposited on Al at zero bias. The fraction of α phase increased with biasing voltage and at 200V pure α phase films were obtained on both Si and Al. In case of Al, with higher

biasing only α phase is observed while pure β phase was obtained on Si at around 200 V biasing, an effect that should be studied further.

The influence of substrate biasing on the crystallographic phase of Ta films was attributed to the effect of energetic ion bombardment of the substrate and the growing film. Deposition with substrate biasing is a type of ion assisted deposition where energetic ions bombarding the surface bring the energy to the film growth process through collisions with the atoms of the growing film. The bombardment leads to increase in mobility and kinetic energy of the surface atoms of the film that may result in the reduction of grain size, lattice expansion, crystal orientation, increased packing density, alteration in surface topography and it also affects the physical properties of the film like adhesion, resistivity and refraction [37]. Ion bombardment leads to removal of weakly bond atoms from the surface and also transfers energy and momentum to the Ta atoms, which may influence the phase of Ta. The observed effects were not due to substrate heating by the ion current, since experiments show that the substrate temperature does not increase above 200°C, while the transition form β to α phase requires 400°C [9].

Another effect of ion bombardment (substrate biasing) was decrease in deposition rate, reflected in film thickness measured by RBS. This effect was attributed to re-sputtering of the film surface by the bombarding energetic ions. The derived sputtering yield of Ta by Ar ions was estimated at approximately 0.5, in agreement with published literature [40].

The results of this study helped in finding conditions and parameters of RF sputtering with substrate bias, which resulted in deposition of α Tantalum phases on aluminum and silicon.

The main conclusions of this study are as under:

- RF magnetron sputtering generates more ions near the substrate than DC magnetron sputtering, resulting in significant substrate ion current such that the fluxes of ions and atoms on the substrate are comparable.

- Substrate ion current increases linearly with increasing RF power but not significantly with increasing substrate bias voltage.

- Ion bombardment of the substrate influences the crystallographic phase of Ta film, as determined by XRD, resulting in deposition of the bcc phase at the substrate bias of approximately 200 V. The effect depends on the substrate and is different in films deposited on aluminum and silicon.

- Ion bombardment of the substrate in the bias sputtering lowers the effective deposition rate by re-sputtering of the growing film.

- This study defined a set of RF sputtering conditions, different than in published literature, for deposition of bcc Ta films desirable in a number of applications.

## APPENDIX A

## CALCULATIONS FOR FILM THICKNESS BASED ON RBS DATA

The calculation used to determine film thickness of Tantalum on Silicon substrate at zero bias is shown below:

$$atoms = 1420\times10^{15}\ atoms/cm^2$$

$$Area(A) = \pi\times(2.75\times2.54)^2\ cm^2$$
$$atoms = \pi\times(2.75\times2.54)^2\times1420\times10^{15}$$
$$= 2.175\times10^{20}\ atoms$$

We have, from the references,

$$6.023\times10^{23}\ atoms \rightarrow 1mole$$
$$1atom \rightarrow \frac{1}{6.023\times10^{23}}\ mole$$
$$2.175\times10^{20}\ atoms \rightarrow \frac{1}{6.023\times10^{23}}\times2.175\times10^{20}\ mole$$
$$\rightarrow 0.3611\times10^{-3}\ mole$$

Again,

$$1mole = 180.92gm$$
$$0.36\times10^{-3}\ mole = 180.92\times0.36\times10^{-3}\ gm$$
$$= 65.13\times10^{-3}\ gm$$
$$= 0.065gm$$

Now let, t = thickness of the film
$\rho$ = density of the material
m = mass of the material

Then,

$$A\times t = \frac{m}{\rho}$$

Substituting the corresponding value,

$$\pi \times (2.75 \times 2.54)^2 \times t = \frac{0.065 gm}{16.6\, gm/cm^3}$$

$$t = \frac{0.065 gm}{16.6\, gm/cm^3 \times \pi \times (2.75 \times 2.54)^2}$$

$$t = 2.55 \times 10^{-5} cm$$

$$t = 255 \times 10^{-9} cm$$

$$t = 255 nm$$

The calculations are made for different samples in a similar way and values are tabulated in chapter 5.

# APPENDIX B

## RBS SPECTRA FOR Ta ON Al AND GLASS SUBSTRATES

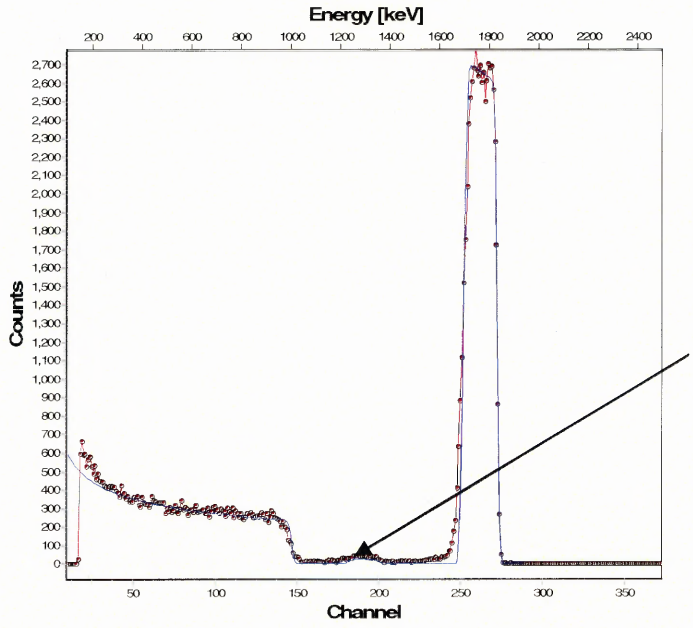


**Figure B.1** RBS Spectra for Ta thin film on Aluminum at -400 V biasing.

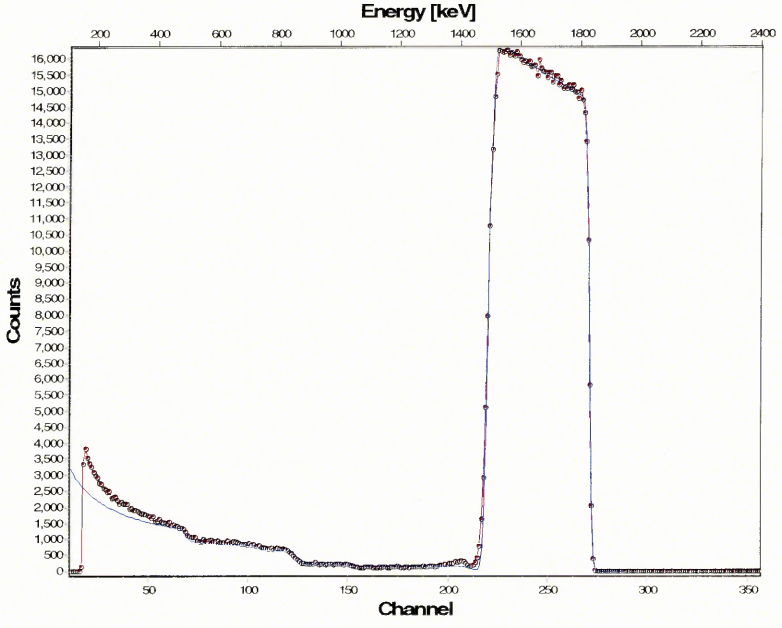


**Figure B.2** RBS Spectra for Ta thin film on Glass at zero biasing.

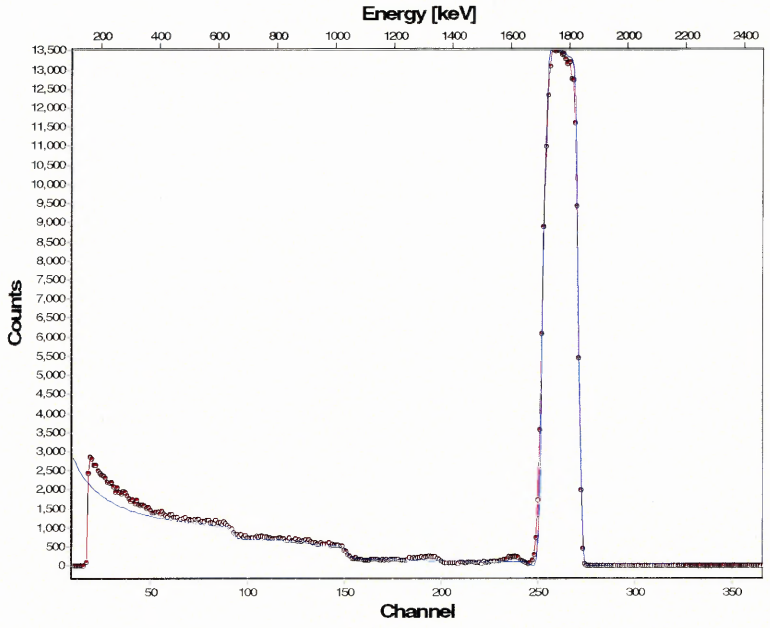


**Figure B.3** RBS spectra for Ta film on Glass at -200 V biasing.

## APPENDIX C

## MEASUREMENT OF MATCHING NETWORK USING VECTOR ANALYZER

### Smith Chart

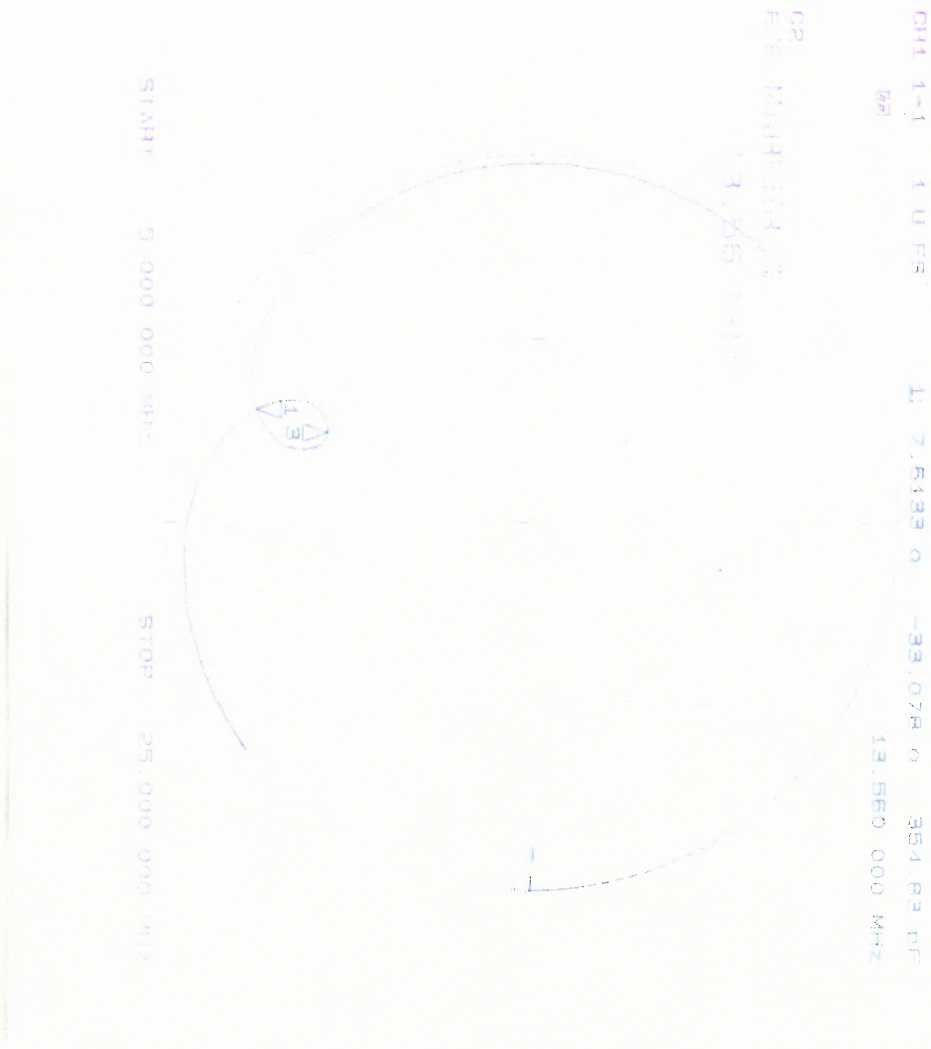

**Figure C.1** Smith chart showing output impedance when input of vector network analyzer is calibrated for 50Ω impedance.

Measurements were performed using vector network analyzer operating at low power (~1 mW) with the vector input impedance to the vector equal to 50 Ω, the output impedance measured was 7.61 Ω – j33.07 Ω at frequency of 13.56 MHz.

**Bode Plot**

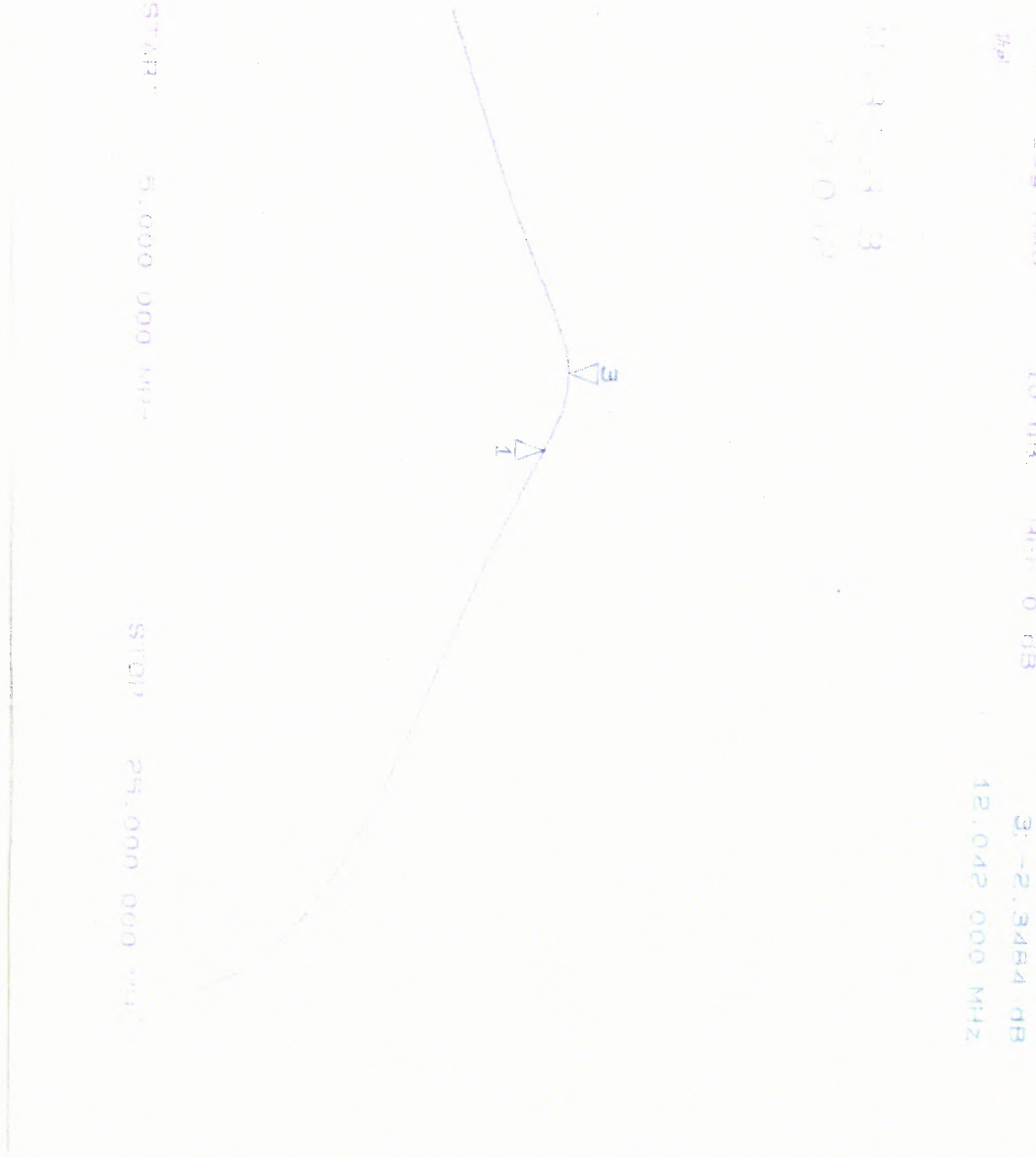

**Figure C.2** Bode plot of the matching network transfer function with markers 1 and 3 set at 13.56 MHz and 12.04MHz respectively.

## REFERENCES


[1] S. L. Lee, M. Doxbeck, J. Mueller, M. Cipollo and P. Cote, "Texture, Structure and Phase Transformation in Sputter Beta Tantalum Coating," *Surf. and Coat. Technology*, 177 - 178, pp. 44 -51, 2004.

[2] S. K. Kim and B. C. Cha: "Deposition of Tantalum Nitride Thin films by DC Magnetron Sputtering," *Thin Solid Films*, 2004.

[3] World Wide Web, http://chemistry.allinfoabout.com/periodic/ta.html (06/14/ 2005).

[4] R. Saha and J. A. Barnard, "Effects of Structure on the Mechanical Properties of Ta and Ta (N) Thin Films prepared by Reactive DC Magnetron Sputtering," *Journal on Crystal Growth,* pp. 495 – 500, 1997.

[5] Y. M. Lu, R. J. Weng, W. S. Hwang and Y. S. Yang, "Study of Phase Transition and Electrical Resistivity of Tantalum Nitride Films prepared by DC Magnetron Sputtering with OES Detection System," *Thin Solid Films*, pp. 356 -360, 2001.

[6] H. B. Nie, S. Y. Wang, L. P. You, C. K. Ong, J. Li and T. Y. F. Liew, "Structural and Electrical Properties of Tantalum Nitride Thin Films fabricated by using Reactive Radio – Frequency Magnetron Sputtering," *Applied Physics and Material Science Processing*, pp. 229 – 236, 2001.

[7] Z. L.Yuan, D. H. Zhang, C. Y. Li, K. Prasad, C. M. Tan and L. J. Tang, "A New Method for Deposition of Cubic Ta Diffusion Barrier for Cu Metallization," *Thin Solid Film,* pp. 126 – 129, 2003.

[8] J. S. Logan, "Control of RF Sputtered Film Properties through Substrate Tuning," *IBM Journal for Research and Development,* pp.172 – 175, March 1970.

[9] L. Gladczuk, A. Patel, C. S. Paur and M. Sosnowski, "Tantalum Films for Protective Coating of Steel," *Thin Solid Films*, pp. 150 – 157, 2004.

[10] L. Gladczuk, A. Patel, J. D. Demaree and M. Sosnowski, "Sputter Deposition of bcc Tantalum Films with TaN under layers for Protection of Steel." *Thin Solid Films*, pp. 295 – 302, 2005.

[11] M. Ohring, "The Materials Science of Thin Films,"Academic Press, 1992.

[12] A. Elshabini and F. D. Barlow III, "Thin Film Technology Handbook," McGraw – Hill, 1997.

[13] K. K. Schuegraf, "Handbook of Thin – Film Deposition Processes and Techniques", Noyes Publication, 1988.

[14] B. Chapman, "Glow Discharge Processes, Sputtering and Plasma Etching," Wiley – Interscience publication, 1980.

[15] G. S. May and S. M. Sze, "Fundamentals of Semiconductor Fabrication," John Wiley and Sons, 2004.

[16] "The Advanced Energy AZX Series Tuner User Manual", June 1994.

[18] Swanson Tatge, Natl. Bur. Stand. (U.S.), Circ. 539,I,29,1953.

[19] P. T. Moseley and C. J. Seabrook, "The Crystal of β – tantalum" *Acta Cryst.*, Sec B, 29, pp. 1170 – 1172, 1973.

[20] N. M. Mazza. "Automatic Impedance Matching System for RF Sputtering," *IBM Journal for Research and Development,* pp.192 – 193, March 1970.

[21] http://www.personal.psu.edu/users/e/e/eeb4/engl202C/propsample2.htm(7-16-2005).

[22] http://www.epanorama.net/documents/wiring/coaxcable.html (7-12-2005).

[23] http://www.corrosionsource.com/handbook/periodic/73.htm (06-14-2005).

[24] A. H. Deutchman and Robert J. Partyka, "Ion Beam Enhanced Deposition," Worthington Beam Alloy Corporation, Ohio.

[25] C. Joshi, "Characterization and Corrosion of bcc-tantalum Coating deposited on Aluminum and Steel substrate by DC Magnetron Sputtering" Thesis presented to *Interdisciplinary Program in Materials Science and Engineering at NJIT*, January, 2003.

[26] R. V. Stuart, "Vacuum Technology Thin Films and Sputtering", Academic Press Inc, 1983.

[27] http://www.rzg.mpg.de/~mam/ (07-20-2005).

[28] P. Verdonck, "Plasma Etching" Retrieved from World Wide Web – http://www.fisicanet.terra.com.br/electronica/Plasm%20Etching.

[29] "The Debye length", Retrieved from World Wide Web - www.physics.sfsu.edu/~lea/courses/grad/**debye**.PDF (07-20-2005).

[30] N. Cheung "Reactive Ion Etching," Retrieved from World Wide Web - www-nst.eecs.berkeley.edu/~ee243/sp05/lectures/Lec_21.pdf (07-17-2005).

[31] A. Patel, "Deposition and Characterization of Magnetron Sputtered bcc-Tantalum" Thesis presented to *Department of Electrical and Computer Engineering at NJIT*, January, 2003.

[32] http://www.probion.fr/tutorial/Sputtering-yield.html (08-01-2005).

[33] C. S. Paur, "Crystallographic Structure and Mechanical properties of Tantalum Coatings on Steel deposited by DC Magnetron Sputtering." Thesis presented to *Interdisciplinary Program in Materials Science and Engineering at NJIT*, August, 2002.

[34] http://home.earthlink.net/~chutko/fundam.htm (08-01-2005).

[35] http://www.cea.com/cai/rbsinst/rinstrum.htm (08-01-2005).

[36] D. W. Matson, E. D. McClanahan, S. L. Lee and D. Windover, "Properties of Thick Sputtered Ta used for protective Gun Tube Coatings." *Surf. and Coat. Technology*, pp. 344-350, 2001.

[37] P. Catania, R. A. Roy and J. J. Cuomo, "Phase formation and Microstructure changes in Tantalum Thin Film Induced by Bias Sputtering." *Journal of Applied Physics,* No.2, pp.1008-1014, July 1993.

[38] K. Ino, T. Shinohara, T. Ushiki and T. Ohmi, "Ion energy, Ion flux and Ion species effects on Crystallographic and Electrical properties of sputter-deposited Ta Thin Film" *Journal of Vacuum. Science. Technol*ogy, Sept/Oct 1997.

[39] C. Cole, "Broadband Antireflection Coatings for Spaceflight Optics," Thesis presented to *Department of Cybernetics, University of Reading*, Sept 1995.

[40] G. K. Vehner and Laegreid N, "Sputtering yields of metals for $Ar^+$ and $Ne^+$ ions with energies from 50 to 600 eV," *Journal of Applied Physics*, volume 32, No.3, pp 365, March 1961.